Reviews

Perovskites by Design: A Toolbox of Solid-State Reactions

Raymond E. Schaak and Thomas E. Mallouk*

*Department of Chemistry, The Pennsylvania State University,
University Park, Pennsylvania 16802*

In recent years, many soft-chemical reactions of layered perovskites have been reported, and they can be classified into sets of similar reactions. Simple ion-exchange and intercalation reactions replace or modify the interlayer cations of layered perovskites, and more complex metathesis reactions replace interlayer cations with cationic structural units. Topochemical condensation reactions that involve dehydration and reduction provide access to a variety of metastable structural features in three-dimensional perovskites, and similar reactions can be used to convert among higher order layered perovskite homologues. Other techniques, such as high pressure and anion intercalation/deintercalation, also yield interesting metastable phases. When combined, the individual reactions complement each other, and a powerful toolbox of solid-state reactions emerges. By using layered perovskites as templates, it is possible to retrosynthetically design new product perovskites that retain the structural features of the precursor layered phases. The toolbox of reactions was used to synthesize a new Ruddlesden−Popper phase, $Na_2Sr_2Nb_2MnO_{10}$, and to demonstrate the first example of a complete cycle of reactions of layered perovskites. In addition, topochemical dehydration and reduction were combined to synthesize the new A-site defective cubic perovskite $Ca_{0.67}Eu_{1.33}La_{0.67}Ti_3O_9$. It should be possible to extend the toolbox to include more complex systems using layer-by-layer assembly of perovskite thin films, which provide access to "made to order" stacking sequences.

Introduction

Solid-state inorganic chemistry thrives on the rich variety of solids that can be synthesized using a wide range of techniques,[1,2] including traditional high-temperature "heat and beat" solid−solid reactions and lower temperature reactions involving hydrothermal[3] and sol−gel[4] synthesis. These techniques are extremely useful and have produced a wide variety of important materials, but serendipity often dominates over rational design and the solid-state chemist can be left with little predictive ability beyond personal experience and intuition. In contrast, organic chemists have access to a large library of reactions that can be applied sequentially to build up complex molecules in predictable ways. Using the tools of retrosynthetic design and convergent synthesis, these reactions provide access to a host of natural products, macromolecules, and supramolecular structures that would otherwise be impossible to make.

There are several synthetic approaches that attempt to create new solids by rational design, and in recent years this area has enjoyed a surge of research activity. Crystal engineering is the purest form of rational design−the molecular precursors are chosen to yield specific structural features (e.g., crystal symmetry, types of bonds, and strengths of intermolecular interactions), and the resulting structure sometimes matches quite closely to what the chemist intended.[5] Many interesting open framework[6] and porous solids that contain large void spaces[7] have been synthesized using these ideas, and the related concept of using secondary building units to assemble more complex systems will certainly yield many important new solids in the future.[8] The dimensional reduction formalism is a useful tool for viewing solids in a predictive way, allowing chemists to decompose a structure into its component parts to form lower dimensional "child" frameworks based on higher dimensional "parent" networks.[9] Thin-film methods such as molecular beam epitaxy,[10] pulsed laser deposition,[11] electrodeposition,[12] and evaporation[13] also provide direct access to complex heterostructures.

Another rational-design approach is that of *chimie douce*, or soft chemistry, which involves the low-temperature modification of existing solid structures to form new solids that retain many of the structural features of the precursor phase.[2,14] Using the principles of soft chemistry, it is possible to synthesize a variety of metastable solids having structures that do not form using more conventional solid-state reactions. Using this approach, solid-state chemists can choose a precursor phase and then design a sequence of low-temperature reactions that will modify the structure in a stepwise process to yield a target product phase. Much like the
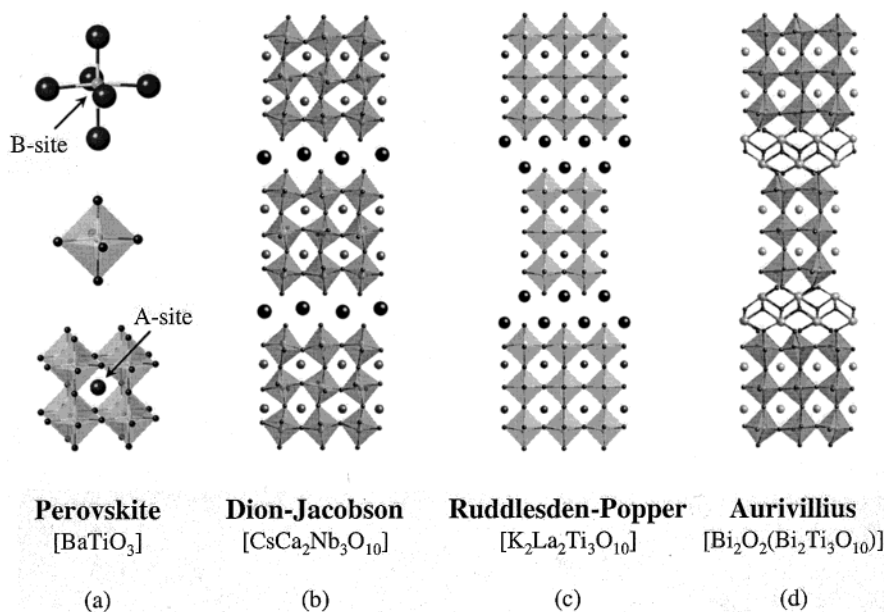
Perovskite	Dion-Jacobson	Ruddlesden-Popper	Aurivillius
$[BaTiO_3]$	$[CsCa_2Nb_3O_{10}]$	$[K_2La_2Ti_3O_{10}]$	$[Bi_2O_2(Bi_2Ti_3O_{10})]$
(a)	(b)	(c)	(d)

Figure 1. Representative structures of selected perovskites and layered perovskites. In (a), the construction of the perovskite unit cell from the corner-sharing BO_6 octahedra is shown. Typical members of the (b) Dion−Jacobson, (c) Ruddlesden−Popper, and (d) Aurivillius families of layered perovskites are also shown. Small black circles represent O, large black circles represent alkali cations, small light circles represent B-site cations, larger shaded circles represent A-site cations, and the light shaded circles in (d) represent Bi.

approach taken by organic chemists, soft chemistry is retrosynthetic in nature. The ultimate goal is to first identify a target structure and then work backward to design a sequence of reactions that will form it from conventional starting materials.

Unfortunately, most demonstrations of a successful soft-chemistry approach involve isolated examples or highly specialized systems in the precursor phase. The ability to generalize a system of soft-chemical approaches to the point where it is feasible to retrosynthetically design an inorganic solid with a variety of useful (and otherwise inaccessible) structural features would be a powerful tool for the solid-state chemist. Such a system would significantly broaden the synthetic tools available in solid-state chemistry, and it would improve our ability to systematically study structure−property relationships in rationally designed materials.

In recent years, there has been a growing interest in using the principles of soft chemistry to design new materials that are based on the perovskite structure. Perovskites are generally metal oxides with the formula ABO_3, where B is a small transition metal cation and A is a larger s-, d-, or f-block cation.[15] In the perovskite structure (Figure 1a), the B-site cation resides in the interstitial site of an octahedron of oxygen anions, and the perovskite unit cell is built from corner-sharing $BO_{6/2}$ octahedra that are connected through B−O−B linkages. The A-site cation fits in the large cavity at the center of eight corner-sharing $BO_{6/2}$ octahedra.

Layered perovskites are intergrowths of perovskite and other structures, and they consist of two-dimensional perovskite slabs interleaved with cations or cationic structural units (Figure 1b−d). The Dion−Jacobson series of layered perovskites, $A'[A_{n-1}B_nO_{3n+1}]$, typified by the $n = 3$ phase $CsCa_2Nb_3O_{10}$ in Figure 1b, has one interlayer cation per formula unit.[16,17] Ruddlesden−Popper phases, $A'_2[A_{n-2}B_nO_{3n+1}]$, such as K_2La_2-Ti_3O_{10} in Figure 1c, have two interlayer cations per

formula unit and possess twice the interlayer charge density of the Dion−Jacobson phases.[18,19] Aurivillius phases, including $Bi_2W_2O_9$ (or $Bi_2O_2[W_2O_7]$ to emphasize the location of the bismuth oxide in the interlayer) shown in Figure 1d, are intergrowths of perovskite and bismuth oxide and have a covalent network of $Bi_2O_2^{2+}$ between the two-dimensional perovskite slabs.[20]

Depending on the choice and stoichiometry of the A- and B-site cations, perovskites and layered perovskites can possess a wide variety of interesting properties including superconductivity,[21] colossal magnetoresistance,[22,23] ferroelectricity,[24] and catalytic activity.[25] Many of the desired structural features of these important materials, such as specific sequences of CuO_2 sheets in superconductors,[26] ordered A- and B-site cations in magnetoresistive materials,[23] texture along the poling direction in ferroelectrics,[24] and spontaneously hydrated interlayer galleries in layered photocatalysts,[27] are often difficult to control thermodynamically.

Soft chemistry offers a potentially powerful alternative for controlling these thermodynamically inaccessible structural and morphological features at the kinetic level.[2,14] In recent years, perovskites have been the target of many low-temperature chemical transformations, and the result is a well-developed system of solid-state reactions. The interlayer cations or structural units of layered perovskites can often be interchanged at low temperatures, which facilitates their subsequent conversion into new phases that are either layered or three dimensionally bonded. Using these reactions, it is now possible to rationally design a variety of interesting structural features into a product perovskite phase using a multistep sequence of low-temperature reactions.

Many of these solid-state reactions are initially demonstrated in a "proof of principle" context, and often the full significance and potential of these reactions go

unrealized. When combined, these individual reactions complement each other, and a powerful toolbox of solid-state reactions emerges. Indeed, one could argue that the individual reactions that make up the toolbox of reactions for perovskites are analogous to the common "name reactions" routinely used by organic chemists. In this review, we present an overview of the reactions that convert layered perovskites into new layered and three-dimensional phases. More importantly, we place these reactions in the context of a series of complementary textbook-style solid-state reactions that can be sequentially applied to retrosynthetically design new perovskites with controlled structural and morphological features.

Overview of Soft Chemistry

While the field of soft chemistry has been reviewed in the past,[2,14] it is beneficial to consider briefly the main principles that underlie the concept of a soft-chemical reaction. First, soft-chemical reactions must preserve most of the bond connectivity of the precursor phase, which means that the structure of the final product closely resembles the structure of the starting material. Thus, ion-exchange, dehydration, and oxidation–reduction chemistry are commonly used techniques. Soft-chemical reactions must also be carried out at a temperature that is sufficiently low to prevent extensive bond breaking and rearrangement of the structural framework. This, in turn, often allows the product to adopt a structure that is kinetically stabilized, providing access to metastable or low-temperature phases that are inaccessible thermodynamically.

In a soft-chemical solid-state reaction, most of the bonds of the solid precursor remain unchanged, so all chemical reactions are carried out at discrete reaction sites within the crystal. Many such reactions involve ion exchange, which interchanges weakly bonded cations and anions in a framework structure. A common example is the exchange of cations in a porous zeolite framework. Another approach is to convert a layered structure into a three dimensionally bonded phase using a topochemical condensation reaction. In this case, selected terminal ligands are removed along a particular crystallographic plane (e.g., removing O^{2-} in combination with H_2 to form H_2O), which serves as a "zipper" to form bonds between parallel planes. For example, the layered titanoniobate $HTiNbO_5$, formed by the exchange of H^+ for the mobile interlayer K^+ cations in the precursor phase $KTiNbO_5$, topochemically dehydrates to form $TiNbO_{4.5}$ (or $Ti_2Nb_2O_9$),[28] which has a three-dimensional framework. Likewise, new forms of binary oxides, such as β-TiO_2[29] and ReO_3-type MoO_3,[30] can be formed by dehydrating the appropriate precursors. A recent example is the elegant single-crystal "zipper" reaction that converts the two-dimensional intermetallic phase $Cs_3Bi_7Se_{12}$ into the three-dimensional phase $CsBi_7Se_{12}$ through a two-step oxidative process.[31]

In this review, we will concentrate on the chimie douce approaches to synthesizing new perovskites. While there are also examples of organic/inorganic[32] and intermetallic perovskite[33] phases that have interesting properties, our focus will be on metal-oxide perovskites because these are the phases for which most of the solid-state reactions have been optimized.

Ion-Exchange Reactions of Layered Perovskites

Ion exchange is the most common low-temperature solid-state reaction of layered perovskites, and it has been used extensively to prepare a wide variety of new layered solids. Figure 2 combines the individual ion-exchange reactions of layered perovskites into a complete set of complementary reactions. Initial inspection of Figure 2 makes clear the ability to easily convert among many types of layered perovskites. In addition, it is possible to synthesize a large number of new layered perovskites with interesting structures and properties simply by exploiting the well-known concept of ion exchange.

Dion–Jacobson phases[16,17] (Figure 2g) were the first reported examples of ion-exchangeable layered perovskites, and the initial ion-exchange reactions involved the replacement of larger interlayer cations such as Cs^+, Rb^+, and K^+ with smaller cations such as Na^+, Li^+, NH_4^+, and Tl^+ (Figure 2h) using molten nitrate salts ($T_m \sim 300$ °C) as the ion-exchange medium.[16,34,35] Dion–Jacobson phases containing small interlayer cations such as Li^+ or Na^+ are often difficult to synthesize as phase-pure materials at traditional reaction temperatures (>1000 °C) where three-dimensional perovskites are usually more stable. Larger cations, such as Cs^+, favor the formation of layered perovskites because Cs^+ fits better in the large interlayer A′-site of a layered perovskite than in the smaller A-site of a three-dimensional perovskite.[36] Smaller cations are often desired between the layers, however, because of the improved ionic conductivity[37,38,39b] and the cation-size considerations that are crucial for subsequent low-temperature reactions.[40] Fortunately, ion exchange provides access to these structures. Divalent ion exchange of Dion–Jacobson phases (not shown) is also possible,[41] although it results in phases that have less than half of the interlayer sites filled. In addition, the exchange efficiencies are often low compared with those involving monovalent exchange.

The interlayer alkali cations of Dion–Jacobson phases can also be replaced with protons by exchange in acid (Figure 2f).[16,42–44] Like many other layered solid acids,[45] the proton forms of most Dion–Jacobson phases are solid acids that intercalate a variety of organic bases (Figure 2i)[42,46] and alcohols.[47] Typically, long-chain alkylamines such as *n*-octylamine form paraffin-like bilayers in the interlayer gallery.[42] Depending on the acidity of the protons attached to the terminal oxygen atoms along the perovskite block, organic bases with a range of pK_b's can intercalate. For example, alkylamines, which typically have pK_b's near 3.4, are readily intercalated into Dion–Jacobson phases such as $HCaLaNb_2TiO_{10}$.[35] Gopalakrishnan and co-workers found that similar reactivity does not occur in $HLa_2Ti_2NbO_{10}$ (derived from $KLa_2Ti_2NbO_{10}$), which has most of its protons attached to TiO_6 octahedra. These are not as acidic as acid sites on NbO_6 octahedra.[35] Interestingly, a recent investigation of the structure of $CsLa_2Ti_2NbO_{10}$ and related phases revealed a unique B-site cation ordering sequence of $(Ti_{0.5}Nb_{0.5})O_{6/2}$–$TiO_{6/2}$–$(Ti_{0.5}Nb_{0.5})O_{6/2}$.[46,48] Accordingly, $HLa_2Ti_2NbO_{10}$ derived from $CsLa_2Ti_2NbO_{10}$ was found to intercalate alkylamines because a sufficient number of protons are attached to NbO_6 octahedra, which enhances the interlayer reactivity.[46]
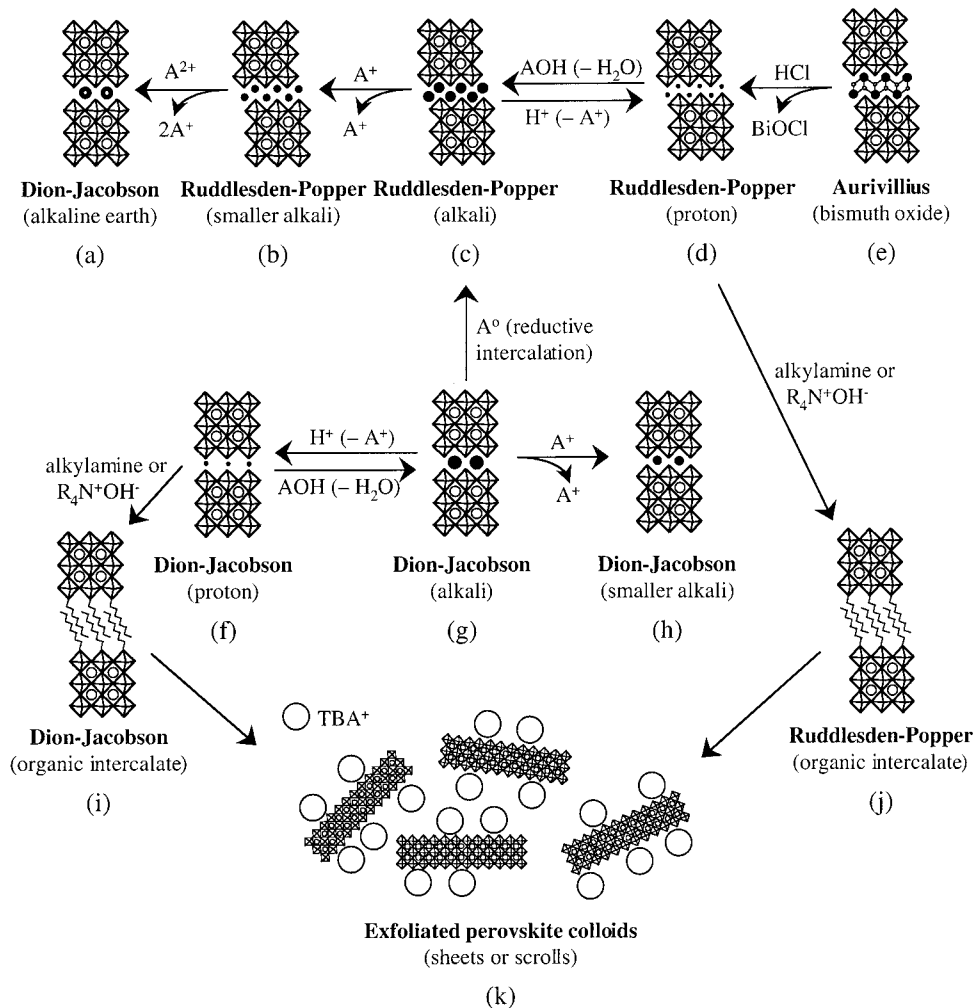
Figure 2. Ion-exchange and intercalation reactions of layered perovskites that involve discrete interlayer cations.

Ruddlesden–Popper phases[18,19] (Figure 2c) also undergo ion-exchange reactions. Like the Dion–Jacobson phases, the interlayer alkali cations of Ruddlesden–Popper phases (typically Na^+, K^+, and sometimes Rb^+) can be replaced by smaller alkali cations such as Na^+, Li^+, NH_4^+, and Ag^+ using molten salt ion-exchange reactions (Figure 2b).[19,38,49,50] Ruddlesden–Popper phases are especially amenable to divalent ion exchange because two interlayer alkali cations can be replaced with one divalent cation to form a Dion–Jacobson phase (Figure 2a). Hyeon and Byeon prepared $M^{II}La_2Ti_3O_{10}$ (M = Co, Cu, Zn) by exchanging $2Na^+$ for M^{2+} using the molten nitrates, chlorides, or eutectic mixtures.[51] We used aqueous ion exchange to form $A^{II}Eu_2Ti_3O_{10}$ (A = Ca, Sr) and $M^{II}Eu_2Ti_3O_{10}$ (M = Ni, Cu, Zn),[40] and Gopalakrishnan and co-workers used a higher temperature metathesis reaction (Figure 3d) to form $A^{II}La_2$-Ti_3O_{10} (A = Sr, Ba, Pb).[52] Protons can also replace the interlayer alkali cations (Figure 2c-d),[19,39c,53–56] which opens up the interlayer gallery to subsequent acid/base reactions.

We recently reported a reaction that converts the proton form of a Ruddlesden–Popper phase into its alkali form (Figure 2d,c).[57] Using this reaction, it is possible to design new Ruddlesden–Popper phases that have larger interlayer cations than those that are normally stable. (Unlike the Dion–Jacobson phases, which often require large interlayer cations to form, the
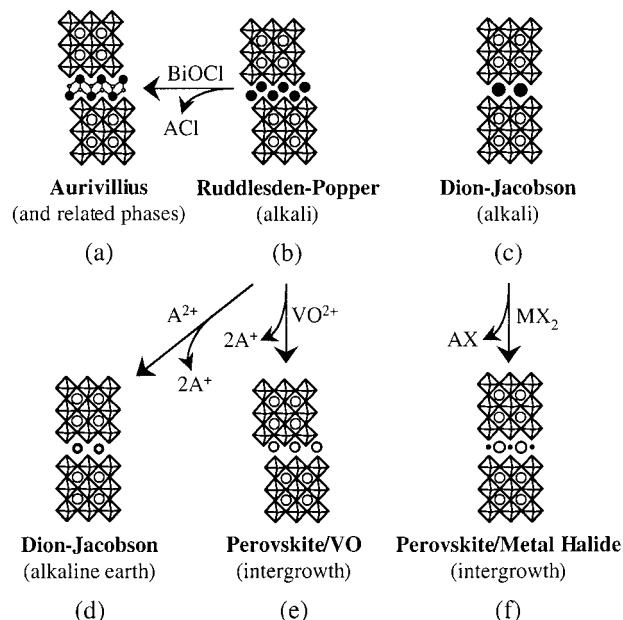

Figure 3. Ion-exchange reactions of layered perovskites that involve replacing interlayer cations with cationic structural units.

interlayer cations of Ruddlesden–Popper phases coordinate with the terminal oxygen atoms of the perovskite block to form a rock-salt-type layer, and larger cations

are usually less stable in such a coordination environment.) For example, $NaLnTiO_4$ (Ln = lanthanide), a series of single-layer Ruddlesden−Popper phases,[39] has a unique ordering of Na^+ and Ln^{3+} cations in alternate layers that depends crucially on both the similar size and different charge of the Na^+ and Ln^{3+} cations. Thus, $KLnTiO_4$ and $LiLnTiO_4$, which have interlayer cations that are larger and smaller than Na^+, respectively, are unstable at the high temperatures needed to synthesize $NaLnTiO_4$. Using $HLnTiO_4$ as a template, we were able to prepare $KLnTiO_4$ (Ln = La, Nd, Sm, Eu, Gd, Dy) by reaction in hot aqueous KOH.[57] ($LiLnTiO_4$ can be prepared by ion exchange of $NaLnTiO_4$ in molten $LiNO_3$[38] or by the acid/base reaction of $HLnTiO_4$ with aqueous LiOH.[58]) $A_2Eu_2Ti_3O_{10}$ (A = Li, Na) could also be synthesized by the reaction of $H_2Eu_2Ti_3O_{10}$ (formed by proton exchange of $K_2Eu_2Ti_3O_{10}$) with hot aqueous AOH.[58] Interestingly, the Dion−Jacobson phase $HCa_2Nb_3O_{10}$ also intercalates alkali cations upon reaction with AOH, but the equilibrium products are substoichiometric (unless the interlayer gallery is first expanded by the pre-intercalation of an alkylamine), and the exchange efficiency depends on the size of the exchanging cation.[59]

While the proton forms of most Dion−Jacobson phases intercalate organic bases,[42] Gopalakrishnan and co-workers initially found that organic bases would not intercalate into the interlayer gallery of Ruddlesden−Popper titanates such as $H_2La_2Ti_3O_{10}$.[60] Presumably, the staggered layers are held together more strongly than those of the Dion−Jacobson phases, which have only half the interlayer charge density. Since then, Sugahara and co-workers synthesized a Ruddlesden−Popper niobate with the nominal composition $H_2SrNaNb_3O_{10}$, and they discovered that the niobate intercalated *n*-butylamine and *n*-octylamine.[61] Likewise, we recently found that Ruddlesden−Popper tantalates such as $H_2CaNaTa_3O_{10}$ and $H_2Ca_2Ta_2TiO_{10}$ also intercalate alkylamines (Figure 2j), suggesting that the barrier to intercalation may be kinetic.[54,62] Thus, compositionally tailoring the acidity of the interlayer protons by incorporating more acidic Ta^{5+} and Nb^{5+} cations into the B-sites of layered perovskites makes it possible to form interesting organic/inorganic hybrid materials by intercalation into both Ruddlesden−Popper and Dion−Jacobson phases.

In general, intercalating long-chain organic bases into layered perovskites (and other layered solid acids) leads to organic/inorganic hybrid solids because the van der Waals forces that arise from the paraffin-like arrangement of the organic chains stabilize the structure.[45] However, intercalation of short-chain amines, such as propylamine, or sterically bulky organic bases, such as tetra-(*n*-butyl)ammonium hydroxide, does not lead to a stable solid because the organic intercalates cannot pack tightly. Instead, the interlayer gallery swells with solvent until the forces that hold the layers together are overcome, and the solid delaminates to form a colloidal suspension of sheets (Figure 2k).[43,62−64] An alternate approach to exfoliation was recently reported by Choy and co-workers,[65] who showed that the triple-layer Dion−Jacobson phase $HCa_2Nb_3O_{10}$ reacts with 6-aminoundecanoic acid (AUA) in its cationic form (at low pH where the amine is protonated) to form the stable

intercalation solid $(AUA)Ca_2Nb_3O_{10}$. As the pH is increased, the carboxylate groups deprotonate and repel the negatively charged perovskite slabs in the bulk solid, forcing the perovskite sheets to exfoliate. Regardless of the method of exfoliation, these colloidal perovskite sheets are essentially nanoscale single-crystal perovskites, and they are interesting building blocks for nanoscale assemblies.

Another important intercalation reaction was reported by Armstrong and Anderson, who demonstrated that the Dion−Jacobson phase $RbLaNb_2O_7$ could be converted into the Ruddlesden−Popper phase $Rb_2LaNb_2O_7$ by reductive intercalation of Rb^0 (Figure 2g−c).[66] In this reaction, rubidium vapor intercalates into the interlayer gallery and adds to the Rb that is already there. In the process, Nb^{5+} is reduced to Nb^{4+} as Rb^0 is oxidized to Rb^+. More recently, Toda and co-workers have elaborated this technique to synthesize reduced tantalate Ruddlesden−Popper phases such as $Na_2Ca_2Ta_3O_{10}$, $Li_2Ca_2Ta_3O_{10}$, and $Li_2LaTa_2O_7$ by reacting the Dion−Jacobson phases $NaCa_2Ta_3O_{10}$, $LiCa_2Ta_3O_{10}$, and $LiLaTa_2O_7$ (formed from the molten-salt ion exchange of the corresponding Rb phases) with NaN_3 and *n*-butyllithium.[67] Recently, Choy and co-workers synthesized $Li_2Bi_4Ti_3O_{12}$ by the reaction of the triple-layer Aurivillius phase $Bi_4Ti_3O_{12}$ with *n*-butyllithium, which indicates that Aurivillius phases are also amenable to reductive intercalation.[68]

The reductive intercalation reaction is significant not only because it converts between two families of layered perovskites but also because it opens the door to valence manipulation because the products have mixed-valent $Nb^{4+/5+}$ and $Ta^{4+/5+}$. Accordingly, reports that suggest the possibility that superconductivity exists in $Na_2Ca_2Ta_3O_{10}$[69] and $Li_xKCa_2Nb_3O_{10}$[70] (formed by reductive intercalation of $KCa_2Nb_3O_{10}$ with *n*-butyllithium) indicate that interesting electronic properties may be possible by exploiting these reactions.

Wiley and co-workers demonstrated a powerful multistep approach for fine-tuning the oxidation state of a B-site cation in a layered perovskite by combining several of the above reactions.[71,72] For example, divalent ion exchange of the Ruddlesden−Popper phase $NaLaTiO_4$ forms $Ca_{x/2}Na_{1-x}LaTiO_4$. Because one Ca^{2+} replaces two Na^+ cations, vacant sites are left in the interlayer gallery.[71] Upon exposure to Na^0, reductive intercalation occurs to form $Na_{1-x+y}Ca_{x/2}LaTiO_4$, where the final oxidation state of Ti is controlled by the number of vacant interlayer sites that can intercalate Na^0.[71] A similar reaction was demonstrated for $Na_{2-x+y}Ca_{x/2}La_2Ti_3O_{10}$, and the products exhibit interesting electron localization effects.[72]

Acid leaching is analogous to ion exchange because it replaces cations or other structural units with protons. Sugahara and co-workers developed an important reaction that converts Aurivillius phases into the proton form of a Ruddlesden−Popper phase by selectively dissolving the interlayer bismuth oxide in acid, which does not attack the perovskite block.[61,73] Upon reaction with HCl, the interlayer $Bi_2O_2^{2+}$ of an Aurivillius phase such as $Bi_2O_2[SrNaNb_3O_{10}]$ is leached and replaced with two protons to form the triple-layer Ruddlesden−Popper phase $H_2SrNaNb_3O_{10}$, which also intercalates organic bases as mentioned earlier.[61]

When the ion-exchange reactions in Figure 2 are combined, it becomes clear how easy it is to design new layered perovskites in a stepwise manner. Using a sequence of reactions taken from Figure 2, one could in principle prepare an Aurivillius phase (Figure 2e) with a B-site cation such as W^{6+} or V^{5+} (which are often found in Aurivillius phases, but have not yet been incorporated directly into the B-sites of Ruddlesden–Popper or Dion–Jacobson phases), and then convert it to the proton form of a Ruddlesden–Popper phase by acid leaching (Figure 2d), which makes it amenable to subsequent acid–base chemistry. As such, the new Ruddlesden–Popper solid acid could be exfoliated to form nanoscale colloidal sheets (Figure 2k), or it could be reacted with base to form a Ruddlesden–Popper phase with interlayer alkali cations (Figure 2c). Likewise, divalent ion exchange could be used to form a new Dion–Jacobson phase (Figure 2e). Thus, using this and related sequences of reactions, it should be possible to synthesize new Ruddlesden–Popper and Dion–Jacobson phases with a variety of B-site and interlayer cations that are not normally stable in such phases.

Ion-Exchange Reactions Involving Interlayer Structural Units

While Figure 2 highlighted the many ion-exchange reactions that place discrete cations between the perovskite layers, Figure 3 focuses on those metathesis reactions that involve replacing the interlayer alkali cations with structural units. Such ion-exchange reactions are interesting because they can convert layered perovskites into intergrowth structures that have more complex stacking sequences.

Wiley and co-workers prepared a new series of perovskite/metal halide intergrowth structures by replacing the interlayer alkali cation of a variety of Dion–Jacobson phases with CuX^+ (X = Cl, Br) by reaction with CuX_2 (Figure 3f).[74] In a typical example, the double-layer Dion–Jacobson phase $RbLaNb_2O_7$ reacts with $CuCl_2$ to form $(CuCl)LaNb_2O_7$ and RbCl, which is a byproduct that can be washed away. $(CuCl)LaNb_2O_7$ and related phases are interesting layered perovskite intergrowths because they contain an interconnected $CuCl^+$ network between the host perovskite layers. The synthetic approach was recently generalized to include a variety of systems. CuX^+ exchanges with several interlayer cations, including Rb^+, K^+, H^+, Li^+, and NH_4^+, and the reaction also works with many Dion–Jacobson phases, including $RbCa_2Nb_3O_{10}$ and $RbLa_2Ti_2$-NbO_{10}.[75] The ion-exchange reaction was further extended to include the co-exchange of $FeCl^+$ by reaction of a Dion–Jacobson phase with $FeCl_2$.[76]

Gopalakrishnan and co-workers independently reported a metathesis reaction that converts the alkali form of a Ruddlesden–Popper phase (Figure 3b) into an Aurivillius phase (Figure 3a) by ion-exchange of $2K^+$ for $Bi_2O_2^{2+}$.[52] For example, the Aurivillius phase $Bi_2O_2[La_2Ti_3O_{10}]$ forms from the solid-state reaction of $K_2La_2Ti_3O_{10}$ with BiOCl. Likewise, a related phase $PbBiO_2[LaNb_2O_7]$ was shown to form from the reaction of $KLaNb_2O_7$ with $PbBiO_2Cl$.[52] The same ion-exchange approach was used to prepare the new Dion–Jacobson phases $A^{II}La_2Ti_3O_{10}$ (A^{II} = Sr, Ba, Pb) upon reaction with ACl_2 (Figure 3d).[52] An interesting perovskite/
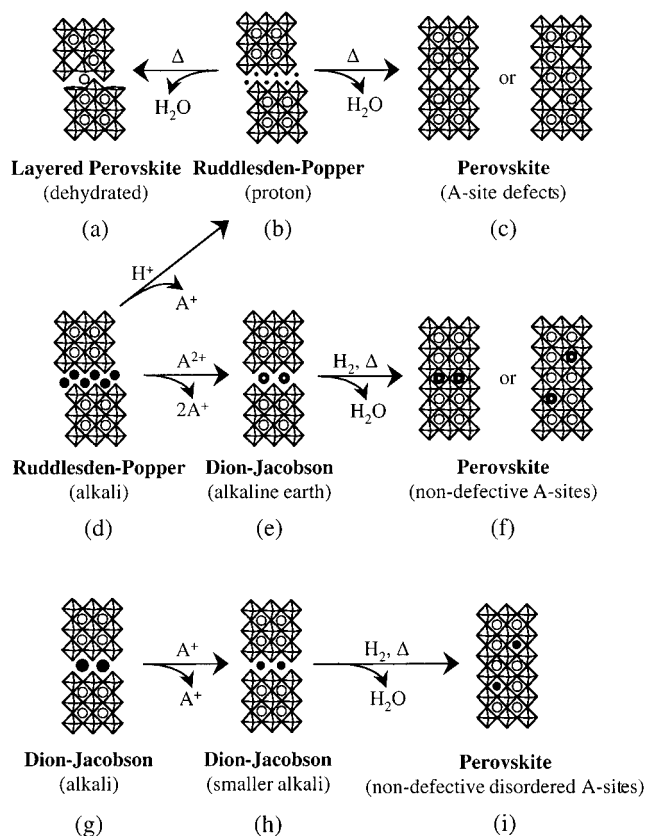

Figure 4. Topochemical condensation reactions, including dehydration (a, c) and reduction (f, i) that convert layered perovskites into three-dimensional phases.

vanadium oxide intergrowth structure was also synthesized by the lower temperature reaction of $K_2La_2Ti_3O_{10}$ with aqueous $VOSO_4$ (Figure 3e).[52]

By combining the metathesis reactions reported by Wiley and Gopalakrishnan, it is evident that one could synthesize a wide variety of new intergrowth structures from both Dion–Jacobson and Ruddlesden–Popper precursors. Using these and related reactions, it may also be possible to synthesize new solids with interesting properties, such as new Aurivillius phases that are ferroelectric or new intergrowth structures that have interesting magnetic properties. Extending these ion-exchange reactions to include other structural units, such as two-dimensional copper oxide or manganese oxide networks, could open the door to new superconductors or magnetoresistive materials.

Topochemical Condensation Reactions

Some of the most interesting low-temperature reactions of layered perovskites involve topochemical condensation, which removes oxygen along the interlayer gallery to form a three-dimensional perovskite. As shown in Figure 4, reactions exist to transform both Ruddlesden–Popper and Dion–Jacobson phases into perovskites with a variety of interesting structural features.

The most common topochemical condensation reaction is dehydration, which removes a row of interlayer oxygen atoms along with their attached protons as water upon heating. While topochemical dehydration has long been used to form new metastable solids (e.g., the synthesis of $Ti_2Nb_2O_9$ from $HTiNbO_5$[28]), Gopalakrish-

nan and Bhat were the first to extend the reaction to perovskites.[19] Upon heating of a Ruddlesden−Popper solid acid such as $H_2La_2Ti_3O_{10}$ (Figure 4b) to between 350 and 500 °C, water is lost along the interlayer gallery, and the $TiO_{6/2}$ octahedra of the perovskite block collapse to form the three-dimensional perovskite $La_2Ti_3O_9$ or $La_{2/3}TiO_3$ (Figure 4c).[19] The product phase has two-thirds of its A-sites filled with La^{3+}, while the other one-third of the A-sites are vacant or defective. Because the La^{3+} cation is large and highly charged, it remains in the original perovskite block, so $La_{2/3}TiO_3$ has ordered A-site cations and defects in the sequence $(La^{3+}-La^{3+}-defect-)_n$. Interestingly, for the smaller lanthanides, dehydration of $H_2Ln_2Ti_3O_{10}$ (Ln = Nd, Sm, Eu, Gd, Dy) does not yield a defective three-dimensional perovskite. Instead, a layered structure with a highly contracted stacking axis is retained upon dehydration,[19,55,77,78] and the layered structure is stabilized by the movement of some of the Ln^{3+} from the perovskite block to the interlayer gallery (Figure 4a).[55] Further heating of $Ln_{2/3}TiO_3$ forms pyrochlore-type $Ln_2Ti_2O_7$.

The double-layer Ruddlesden−Popper phase $H_2SrTa_2O_7$ also topochemically dehydrates to form the defective perovskite $SrTa_2O_6$, which has only half of the A-sites filled.[53,56] Unlike $La_2Ti_3O_9$, which retains the A-site ordering of La^{3+} that was present in the layered precursor, Sr^{2+} is randomly distributed among the available A-sites of the perovskite lattice. Apparently, the higher charge of La^{3+} provides a sufficient barrier to disordering, while the lower charge of Sr^{2+} allows it to move into the vacant sites at the temperature required for the dehydration reaction to occur. We recently found that the triple-layer Ruddlesden−Popper tantalates and titanotantalates $H_2CaNaTa_3O_{10}$, $H_2Ca_2Ta_2TiO_{10}$, and $H_2SrLaTi_2TaO_{10}$ also topochemically dehydrate to form the disordered, A-site defective phases $CaNaTa_3O_9$, $Ca_2Ta_2TiO_9$, and $SrLaTi_2TaO_9$, respectively.[54]

Most Dion−Jacobson phases are usually not susceptible to topochemical dehydration because they have only half the number of interlayer protons than are necessary to remove a row of oxygen atoms from the lattice upon dehydration. However, $HCa_2Nb_3O_{10}$ was found to partially dehydrate to $Ca_4Nb_6O_{19}$, and the proposed structural model contains a buckled interlayer arrangement where only half of the octahedra condense, while the others remain separated.[79] Upon further heating, $Ca_4Nb_6O_{19}$ decomposes to a mixture of $CaNb_2O_6$ and $Ca_2Nb_2O_7$.

An alternate approach for condensing a Dion−Jacobson phase into a three-dimensional perovskite is to introduce extra hydrogen into the interlayer gallery, which can then combine with oxygen to fully dehydrate.[40,80] To accomplish this, the cations in the perovskite block must be easily reducible so that upon intercalation, H_2 can be oxidized as a perovskite-block cation is reduced. While others have used Ti^{4+}, Nb^{5+}, and Ta^{5+} as cations that can be reduced upon reaction with Na^0 or *n*-butyllithium, we chose to incorporate the easily reducible Eu^{3+} cation into the A-sites of the layered perovskite. When heated in hydrogen, Eu^{3+} reduces to Eu^{2+}, which forces the removal of oxygen from the perovskite block and facilitates the bridging of the octahedra to form a three-dimensional perovskite.

Because the condensation occurs when hydrogen is introduced into the interlayer gallery, the perovskite slabs can collapse on top of any cation that is already in the interlayer A′-site of a Dion−Jacobson phase, such as Na^+ or Ca^{2+}. Using this approach, it is possible to synthesize nondefective three-dimensional perovskites that have ordered or disordered A-site cations.

The triple-layer Dion−Jacobson phase $CsEu_2Ti_2NbO_{10}$ (Figure 4g) can be converted to $AEu_2Ti_2NbO_{10}$ (A = Na, Li) through molten salt ion exchange (Figure 4h) and then heated in hydrogen to reduce Eu^{3+} to Eu^{2+} and bridge the octahedra to form the nondefective perovskite $AEu_2Ti_2NbO_9$ (Figure 4i).[40] Because Na^+ and Li^+ are monovalent and relatively small, they can disorder along with Eu^{2+} among the A-sites of the perovskite lattice. (Eu^{2+} is approximately the same size as Sr^{2+}, which also disorders among the perovskite A-sites in the lower temperature topochemical dehydration of $H_2SrTa_2O_7$.[53,56])

Using a set of reactions initially presented in Figure 2, Ruddlesden−Popper phases (Figure 4d) can be converted into Dion−Jacobson phases by divalent ion exchange (Figure 4e). For example, the triple-layer Ruddlesden−Popper phase $K_2Eu_2Ti_3O_{10}$ forms $A^{II}Eu_2Ti_3O_{10}$ (A^{II} = Ca, Sr) by reaction in aqueous $A^{II}(NO_3)_2$, and subsequent reduction in hydrogen forms the three-dimensional perovskite $A^{II}Eu_2Ti_3O_9$ (Figure 4f).[40] Interestingly, the charge and size of the A^{2+} cations provide a sufficient barrier to disordering, so the Eu^{2+} and A^{2+} cations in $A^{II}Eu_2Ti_3O_9$ remain ordered. Thus, this approach provides a route to A-site ordered nondefective perovskites that are inaccessible by other synthetic techniques.

$M^{II}Eu_2Ti_3O_{10}$ (M^{II} = Ni, Cu, Zn), formed by divalent ion exchange of $K_2Eu_2Ti_3O_{10}$ using aqueous $M^{II}(NO_3)_2$, can also be topochemically reduced in hydrogen to form perovskite-type $M^{II}Eu_2Ti_3O_9$.[40] Unlike $A^{II}Eu_2Ti_3O_9$, the final product has disordered A-site cations (Figure 4f), which indicates that the smaller M^{2+} cations are susceptible to moving around the A-sites of the perovskite lattice. Interestingly, A-site ordered $M^{II}Eu_2Ti_3O_9$ is observed at intermediate stages of the reaction,[40] which argues that the final disordered product is the thermodynamically stable form of the ordered phase that forms initially. Apparently, by tailoring the charge and size of the interlayer cations in the layered precursor, one can control the ordering of the A-site cations in the final product.

Topochemical condensation reactions can also be applied to the synthesis of layered perovskites that are novel higher order homologues of existing lower order layered phases (Figure 5). For example, Gopalakrishnan and co-workers found that $Ln_2\square Ti_2O_7$ (Ln = La, Nd, Sm, Gd), an A-site defective double-layer series of Ruddlesden−Popper phases (Figure 5c) could be synthesized by the controlled dehydration of the single-layer series $HLnTiO_4$ (Figure 5b), which is first formed by acid exchange of $NaLnTiO_4$ (Figure 5a).[81] Likewise, we found that divalent ion exchange of $NaEuTiO_4$ (Figure 5a) forms $Ca_{0.5}EuTiO_4$ (Figure 5d), which can be topochemically reduced in hydrogen to form $Ca_{0.5}EuTiO_{3.5}$ or $Eu_2CaTi_2O_7$ to emphasize the fact that it is a nondefective double-layer Ruddlesden−Popper phase (Figure 5e).[80] The intermediate phase, $Ca_{0.5}EuTiO_4$ or $CaEu_2Ti_2O_8$, is

Figure 5. Topochemical condensation reactions that convert layered perovskites into high-order layered homologues.

an interesting mixed Ruddlesden–Popper/Dion–Jacobson phase with alternating staggered and eclipsed layers (Figure 5d), and it can be considered as an intergrowth of the two structures.[80]

Topochemical dehydration and reduction are powerful complementary approaches for controlling the defect structure and ordering of A-site cations in product perovskite phases. A variety of three-dimensional perovskites have been synthesized from layered precursors using these techniques, and the reactions are sufficiently generalized to begin designing product phases that have more complex structural features. Because the electronic properties change as the dimensionality of the solid network changes, the topochemical condensation reactions could offer a way to fine-tune properties. For example, magnetoresistance and superconductivity occur in both layered and three-dimensional perovsites, but their properties and Curie temperatures vary depending on the dimensionality.[21,23] Likewise, the magnetoresistive properties of the Ruddlesden–Popper series $(La,Sr)_{n+1}Mn_nO_{3n+1}$ vary with n or the number of octahedra that stack in the perovskite block.[23] By converting among different homologues in a series of layered perovskites, one could imagine fine-tuning such properties.

Other Structural Transformations of Perovskites

The reactions presented up to this point have dealt primarily with ion-exchange and topochemical condensation reactions. There are, however, several important examples of structural transformations in perovskites that do not necessarily fit into the above categories. For example, there are high-pressure techniques that convert layered perovskites into three-dimensional phases without requiring any interlayer condensation reactions.[82,83] Low-temperature oxygen intercalation and

deintercalation reactions[84–86] as well as fluorine insertion reactions[87–89] can be used to synthesize interesting phases that are inaccessible by other routes. Finally, there are multistep intercalation reactions of layered superconductors that probe the nature of superconductivity as well as open the door to new organic/inorganic hybrid superconductors.[90–92]

Byeon and co-workers transformed a layered perovskite directly into a nondefective three-dimensional perovskite using a high-pressure technique rather than a condensation reaction.[82] While this approach does not require reducible cations in the layered precursor, it instead requires anion vacancies in the perovskite block. Gopalakrishnan and co-workers found several years ago that $RbLaSrNb_2M^{II}O_9$ forms a layered perovskite, even though it has the ABO_3 (or $A_3B_3O_9$) stoichiometry, while $ALaSrNb_2M^{II}O_9$ (A = K, Na) forms a three-dimensional perovskite as expected.[36] The large Rb^+ cation favors the formation of a layered structure, and the incorporation of M^{2+} cations into the B-sites of the layered phase creates anion vacancies in the perovskite lattice to maintain charge balance.[36] Because $RbLaSrNb_2M^{II}O_9$ has both the ABO_3 stoichiometry and anion vacancies, Byeon and co-workers recently discovered that it is possible under high pressure to form the stable three-dimensional perovskite phases of the same stoichiometry.[82] Interestingly, some of the $RbLaSrNb_2M^{II}O_9$ (M^{II} = Mg, Cu, Zn) phases remain cubic, while others have a tetragonal distortion, depending on the choice of the M^{2+} cation.[82] This approach could possibly be generalized to other phases to produce a variety of metastable perovskite phases at high pressures.

Poeppelmeier and co-workers recently reported the synthesis of $La_4Cu_3MoO_{12}$, which under ambient conditions is a hexagonal layered perovskite containing cations in unusually low coordination environments.[83] Because high pressure increases the coordination preferences of the cations, $La_4Cu_3MoO_{12}$ transforms to a three-dimensional perovskite at 6 GPa and 1200 °C.[83] The transformation is reversible, and upon heating of the high-pressure form to 800 °C at ambient pressure, the hexagonal layered phase is restored. Interestingly, the high-pressure form of $La_4Cu_3MoO_{12}$ adopts an ordered arrangement of $CuO_{6/2}$ and $(Cu/Mo)O_{6/2}$ octahedra.[83] As such, the structure contains copper–oxygen planes that are not mixed with other cations, which is interesting from a superconductivity perspective.

Most structural transformations of perovskites deal with the transformation of a layered perovskite into a three-dimensional phase, but there is an important example of the opposite approach. Rosseinsky and co-workers recently developed a new topochemical reduction technique that uses oxygen deintercalation in a cubic perovskite to form a highly metastable layered phase.[84,85] The Ni(III) perovskite $LaNiO_3$ is reduced to the Ni(I) layered perovskite $LaNiO_2$ upon reaction with solid NaH near 200 °C.[84] The use of NaH as a reducing agent is crucial to the success of this reaction because higher temperatures are typically required to synthesize reduced compounds such as $LaNiO_2$, which are unstable at such temperatures. Interestingly, the structure of $LaNiO_2$ is analogous to that of the "infinite layer" cuprates, and the isolation of Ni(I) in an isostructural compound could prove useful for understanding super-
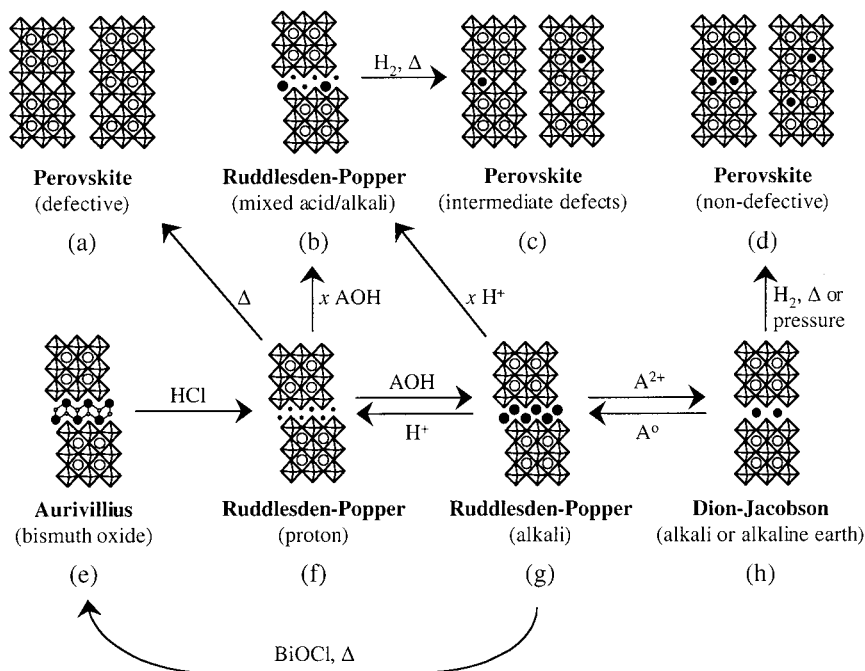
Figure 6. The combined toolbox of solid-state reactions for perovskites, including ion exchange, topochemical dehydration, and topochemical reduction.

conductivity in the cuprates and related materials.[84]

The use of NaH as a powerful reducing agent was also extended to the synthesis of highly reduced cobalt oxides.[85] In this example, Hayward and Rosseinsky show that the $n = 1$ Ruddlesden–Popper phase LaSrCoO$_4$, which contains Co^{3+}, could be reduced to LaSrCoO$_{3.5-x}$ by reaction with solid NaH.[85] While similar phases form from the reduction of LaSrCoO$_4$ with H$_2$ at higher temperatures, the reaction with NaH is superior in its reducing power. In the reduced phase, there is a mixture of Co^{2+} and Co^{1+}, and the high concentration of Co^{1+} in LaSrCoO$_{3.5-x}$ prepared using NaH is unusual in an oxide environment.

In addition to the sodium hydride method, several other chimie douce methods exist for intercalating or deintercalating oxygen in perovskite-type solids.[86] For example, electrochemical oxidation can be used to form La$_2$NiO$_{4+\partial}$ from the $n = 1$ Ruddlesden–Popper phase La$_2$NiO$_4$, and similar results are obtained for the La$_2$CuO$_4$ system.[86] Electrochemical reduction is useful in removing oxygen from a perovskite lattice such as La$_{2-x}$Ba$_x$CuO$_{4+\partial}$, which typically has oxygen overstoichiometry.[86] Chemical reduction using borohydride solution is a powerful technique for preparing oxide nanoparticles and framework solids such as A$_x$WO$_3$ (A = Li, Na, K, NH$_4$), which intercalates cations into the vacant A-sites upon reduction with ABH$_4$.[86,93]

Fluorination methods are intriguing for preparing new oxyfluoride perovskites that often have enhanced properties. Greaves and co-workers prepared the superconductor Sr$_2$CuO$_2$F$_{2+\partial}$ by fluorine insertion into Sr$_2$CuO$_3$, and the fluorine plays an important structural role in the superconductivity.[87] Since then, many other perovskite oxyfluorides have been synthesized using low-temperature fluorination reactions, and it appears that this is a generalized approach to fine-tuning the structure and properties of superconducting materials.[88] Recently, this fluorination approach was extended to

Ruddlesden–Popper manganates, resulting in the novel staged oxyfluoride LaSrMnO$_4$F.[89] This approach could lead to interesting new magnetoresistive materials because fluorine insertion is accompanied by a change in the oxidation state of the B-site manganese.

Choy and co-workers have applied several interesting low-temperature reactions to layered perovskite superconductors to study the two-dimensional nature of superconductivity.[90–92] The high-T_c cuprate superconductors Bi$_2$Sr$_2$Ca$_{m-1}$Cu$_m$O$_y$ ($m = 1$, 2) contain weakly bound Bi$_2$O$_2$ double layers between the copper oxide sheets, and although these interlayer galleries are not ion-exchangeable, they are amenable to intercalation by HgI$_2$.[91] Long-chain organic molecules are then intercalated by the reaction of HgI$_2$[Bi$_2$Sr$_2$Ca$_{m-1}$Cu$_m$O$_y$] with alkylpyridinium iodide, PyC$_n$H$_{2n+1}$I ($n = 1$, 2, 4, 6, 8, 10, 12).[91] Upon intercalation, the stacking axis of the superconductor expands to accommodate the organic intercalate, yet superconductivity is retained in the organic/inorganic hybrids. This provides evidence for the two-dimensional nature of superconductivity in the cuprate superconductors. Interestingly, the hybrid superconductors can also be exfoliated into nanoscale colloidal sheets, and they have been spin-coated to form superconducting thin films.[92]

The Toolbox of Solid-State Reactions

Each of the reactions in Figures 2–5 represents a synthetic tool to use in rationally designing new perovskites. When these individual reactions are combined, a powerful toolbox of solid-state reactions emerges. The previous sections highlighted several sets of low-temperature reactions of layered perovskites, grouped according to similar types of reactions. In Figure 6, we combine some of the most powerful reactions from the previous sets to form a toolbox of reactions for retrosynthetically designing new perovskites.

As already noted, it is possible to transform layered perovskites into three-dimensional perovskites using topochemical dehydration and reduction reactions, and often the product phases have interesting structural features, including A-site defects and ordered A-site cations. Figure 6 shows that one could theoretically convert a Dion–Jacobson, Ruddlesden–Popper, or Aurivillius phase into a three-dimensional perovskite with structural features that resemble the precursor using a multistep sequence of reactions.

Using this approach, it should be possible to take advantage of the unique structural features of each of the types of precursor phases in designing a product phase. For example, Dion–Jacobson phases typically have monovalent cations between the layers, and they yield product phases with monovalent A-site cations that disorder among the perovskite lattice sites. Thus, it may be possible to design new ionic conductors by placing small monovalent cations in the A-sites of the product perovskite lattice. Likewise, some Dion–Jacobson phases were recently found to have ordered B-site cations (Ti^{4+} and Nb^{5+}/Ta^{5+}),[48] and this ordering could be retained in a product perovskite phase. Ruddlesden–Popper phases have twice the interlayer charge density of the Dion–Jacobson phases, so they provide access to three-dimensional phases that have divalent A-site cations that can remain ordered in the perovskite lattice. By introducing d^n ($n > 0$) cations into the B-sites of ion-exchangeable layered perovskites, it may be possible to design new electronic or magnetic materials that have ordered sequences of A- and/or B-site cations. Electronically active B-site cations could be incorporated directly into the parent Ruddlesden–Popper phase, as in $Na_2La_2Ti_{3-x}Ru_xO_{10}$[94] and $Na_2Ln_2Ti_{3-x}Mn_xO_{10}$ (Ln = Sm, Eu, Gd, Dy),[50] or by topochemical methods such as the reductive intercalation of a Dion–Jacobson phase, as in the synthesis of $Rb_2LaNb_2O_7$ from $RbLaNb_2O_7$.[66] Finally, Aurivillius phases are more covalent than their Ruddlesden–Popper and Dion–Jacobson counterparts, so they can stabilize small, highly charged B-site cations such as W^{6+}, Mo^{6+}, and V^{5+}.[20,95] By starting with Aurivillius phases, it may be possible to expand the choice of interesting electronic or magnetic cations in designing new perovskites that yield interesting properties.

It is also possible to form mixed alkali/alkaline earth or acid/alkali Ruddlesden–Popper phases by controlled substoichiometric ion exchange. For example, Wiley and co-workers found that $Ca_{x/2}Na_{1-x}LaTiO_4$ and $Ca_{x/2}Na_{2-x}La_2Ti_3O_{10}$ are single-phase solid solutions.[71,72] Recently, we found that $H_2Eu_2Ti_3O_{10}$ reacts with x equiv of NaOH to form $Na_xH_{2-x}Eu_2Ti_3O_{10}$, and the solid solution exists over the entire range of $0 \leq x \leq 2$, as determined by powder X-ray diffraction and elemental analysis.[96] By controlling the interlayer alkali content, it is possible to synthesize new three-dimensional perovskite phases that have intermediate numbers of defects (see next section). The ability to vary the stoichiometry of a layered perovskite solid solution during ion exchange allows one to superimpose A-site filling control and structural control to design product phases with a complex combination of interesting structural features and defect sites.

One other powerful consequence of the toolbox of reactions is the complete cycle of reactions represented by Figure 6e–g. This cycle indicates that one can convert among Aurivillius phases and both the proton and alkali forms of Ruddlesden–Popper phases. In principle, one could begin with an Aurivillius phase, convert it to a Ruddlesden–Popper solid acid by leaching the $Bi_2O_2^{2+}$, and then react it with AOH to form an alkali Ruddlesden–Popper phase, which could subsequently be reacted with BiOCl to form the Aurivillius phase that was the original starting material. While obtaining starting material after three reactions is typically undesirable, it proves a useful concept. One could begin at any point along the cycle of reactions and obtain any of the other phases by using only a few well-characterized reactions.

Applying the Toolbox—Synthesis of New Perovskites with Controlled Structures

While many examples in the literature have demonstrated the success of the reactions presented thus far, their true power lies in the ability to combine them to predictably design new phases. As we have seen, these reactions work well individually and on selected examples, but they can also be generalized to new systems to yield similar results. Indeed, these reactions are complementary, and they work well together. The solid-state toolbox of reactions can be used quickly and easily to design new layered and three-dimensional perovskites, and its success rate is high. To show how easily and successfully one can design product phases using multistep sequences of reactions, we provide new examples of the use of solid-state retrosynthesis in preparing new perovskites with interesting structural features that are derived from the precursor phases.

A Cycle of Solid-State Reactions—Synthesis of New B-Site Ordered Ruddlesden–Popper Phases. One of the most important reactions for converting among layered perovskites is the acid leaching of the $Bi_2O_2^{2+}$ sheets from an Aurivillius phase to form a Ruddlesden–Popper solid acid. It has been suggested that this reaction will provide access to ion-exchangeable layered perovskites that contain B-site cations not normally seen in such phases, but to date this reaction has only been demonstrated on niobates[61] and tantalates,[73] which are already commonly incorporated into many layered perovskites. In an effort to generalize this reaction, we synthesized $H_2Sr_2Nb_2MnO_{10}$ and Na_2Sr_2-Nb_2MnO_{10}, new Ruddlesden–Popper phases containing ordered B-site Nb^{5+} and Mn^{4+}. These phases have structural features that cannot be directly incorporated into ion-exchangeable layered perovskites.

Recently, Yu et al. reported the synthesis of the triple-layer Aurivillius phase $Bi_2O_2[Sr_2Nb_2MnO_{10}]$, which they found by Rietveld analysis to have ordered B-site cations in the sequence $Nb^{5+}-Mn^{4+}-Nb^{5+}$.[97] The XRD pattern for $Bi_2O_2[Sr_2Nb_2MnO_{10}]$, which matches the reference pattern by Yu et al.,[97] is shown in Figure 7a. By applying the room-temperature acid leaching reaction reported by Sugahara and co-workers,[61] we were able to convert $Bi_2O_2[Sr_2Nb_2MnO_{10}]$ into $H_2[Sr_2Nb_2MnO_{10}]$,[98] a triple-layer Ruddlesden–Popper solid acid (Figure 7b). We then applied the ion-exchange reaction for converting the proton form of a Ruddlesden–Popper phase into
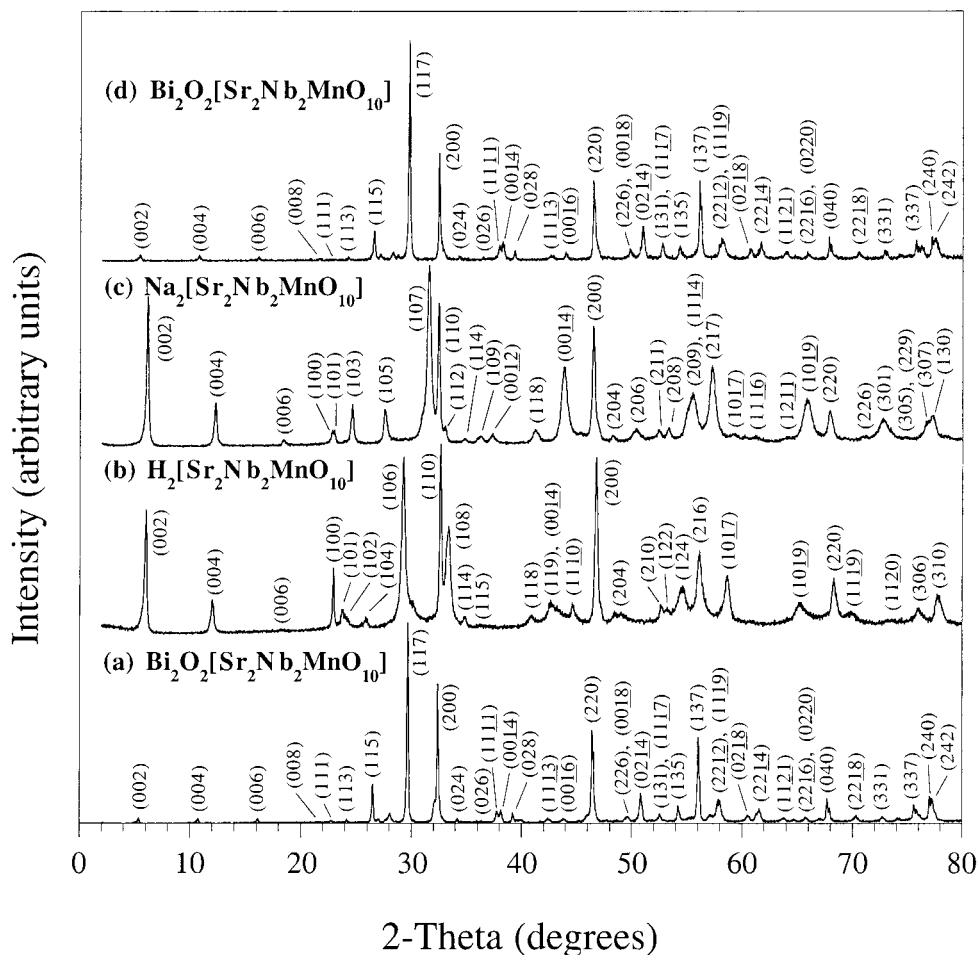
Figure 7. X-ray diffraction patterns for the cycle of solid-state reactions, which includes (a) the Aurivillius phase $Bi_2O_2[Sr_2Nb_2MnO_{10}]$ synthesized as described in ref 98, the Ruddlesden−Popper solid acid $H_2[Sr_2Nb_2MnO_{10}]$, the Ruddlesden−Popper alkali phase $Na_2[Sr_2Nb_2MnO_{10}]$, and the Aurivillius phase $Bi_2O_2[Sr_2Nb_2MnO_{10}]$ synthesized by the reaction of $Na_2[Sr_2Nb_2MnO_{10}]$ with BiOCl.

its alkali form to synthesize $Na_2[Sr_2Nb_2MnO_{10}]$,[99] an ion-exchangeable alkali Ruddlesden−Popper phase (Figure Gc).[100] While $Na_2[Sr_2Nb_2MnO_{10}]$ is stable to above 700 °C, $H_2[Sr_2Nb_2MnO_{10}]$ begins decomposing at 500 °C. Attempts to synthesize $A_2Sr_2Nb_2MnO_{10}$ (A = Li, Na, K, Rb) directly were unsuccessful. Considering the thermal data and data from energy-dispersive X-ray spectroscopy (EDS) that shows stoichiometric ion exchange of Na^+ for H^+, it is evident that $Na_2[Sr_2Nb_2MnO_{10}]$ was formed as expected and is more stable than its proton analogue. Upon reaction with a stoichiometric amount of BiOCl at 800 °C, $Na_2[Sr_2Nb_2MnO_{10}]$ is converted back into $Bi_2O_2[Sr_2Nb_2MnO_{10}]$, and its XRD pattern (Figure 7d) matches that of the original starting phase (Figure 7a).

The reaction sequence in Figure 7 represents the first example of a cyclic solid-state transformation of layered perovskites, and it demonstrates the applicability of the toolbox of solid-state reactions. Assuming that the B-site cation ordering sequence of $Bi_2O_2[Sr_2Nb_2MnO_{10}]$ is preserved in the product Ruddlesden−Popper phases, which is reasonable considering the low-temperature (<45 °C) of the reactions, this multistep approach offers a route to ordered B-site cations in ion-exchangeable Ruddlesden−Popper phases. Up until now, this cation ordering sequence has only been observed in the $Na_2La_2Ti_{3-x}Ru_xO_{10}$ system.[94] We are currently analyz-

ing the detailed structure and magnetic properties of the product Ruddlesden−Popper phases.

Combining Topochemical Dehydration and Reduction−Synthesis of a New Defective Perovskite. Topochemical dehydration of $H_2La_2Ti_3O_{10}$ yields an A-site defective three-dimensional perovskite,[19] while topochemical reduction of $CaEu_2Ti_3O_{10}$ yields a nondefective three-dimensional perovskite with ordered A-site cations.[40] Thus, by combining topochemical dehydration and reduction of an appropriate precursor phase, it should be possible to synthesize a product perovskite with an intermediate number of A-site defects.

To explore this possibility, we synthesized a Ruddlesden−Popper phase with a mixture of Eu^{3+}, which is easily reduced to Eu^{2+} when heated in hydrogen, and La^{3+}, which is not reducible. Reduction of Eu^{3+} will remove some oxygen from the lattice as in the synthesis of $CaEu^{II}_2Ti_3O_9$ from $CaEu^{III}_2Ti_3O_{10}$,[40] but not enough to effect complete condensation. By also incorporating protons into the layered precursor, the remainder of the oxygen can be removed by dehydration. For example, in the solid solution $Na_2Eu_xLa_{2-x}Ti_3O_{10}$, reduction of Eu^{3+} to Eu^{2+} in hydrogen would remove only $x/2$ oxygen atoms per unit cell, which is not sufficient for topochemical condensation to occur. However, if we also include $2-x$ protons per unit cell, dehydration would remove the remaining $(2 - x)/2$ oxygen atoms for a total
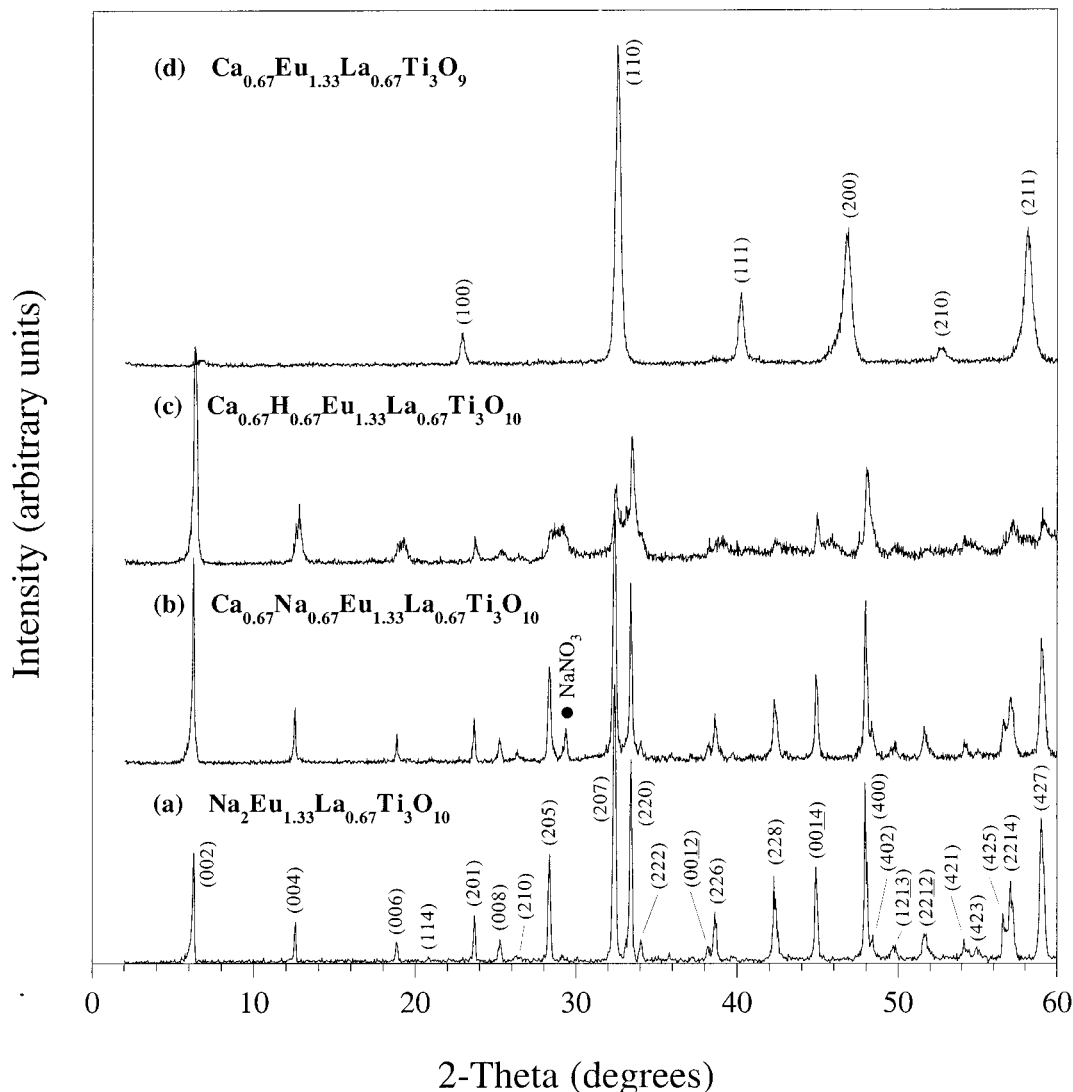
Figure 8. X-ray diffraction patterns for (a) $Na_2Eu_{1.33}La_{0.67}Ti_3O_{10}$, (b) $Ca_{0.67}Na_{0.67}Eu_{1.33}La_{0.67}Ti_3O_{10}$ formed by divalent ion exchange of (a), (c) $Ca_{0.67}H_{0.67}Eu_{1.33}La_{0.67}Ti_3O_{10}$ formed by leaching the sodium in (b) with acid, and (d) the three-dimensional perovskite $Ca_{0.67}Eu_{1.33}La_{0.67}Ti_3O_9$ formed by combining topochemical dehydration and reduction.

loss of $[x/2 + (2 - x)/2]$, or one oxygen atom per unit cell, and topochemical condensation could then occur.

The XRD pattern for the $x = 1.33$ member, $Na_2Eu_{1.33}$-$La_{0.67}Ti_3O_{10}$ [tetragonal, $a = 7.5823(6)$, $c = 28.253(1)$], is shown in Figure 8a. For $Na_2Eu_{1.33}La_{0.67}Ti_3O_{10}$, reduction of Eu^{3+} to Eu^{2+} would remove only 0.67 oxygen atoms per unit cell, and dehydration could be used to remove the remaining 0.33 oxygen atoms to form a three-dimensional perovskite with a nominal $A_3B_3O_9$ stoichiometry. An appropriate precursor phase, such as $A_yH_{0.67}Eu_{1.33}La_{0.67}Ti_3O_{10}$, can be formed using a multistep ion-exchange approach. Borrowing from the approach of Wiley and co-workers,[71,72] we first used divalent ion exchange of $Na_2Eu_{1.33}La_{0.67}Ti_3O_{10}$ to form $Ca_{0.67}Na_{0.67}Eu_{1.33}La_{0.67}Ti_3O_{10}$ [tetragonal, $a = 7.5841$-(4), $c = 28.268(1)$],[101] which is shown in Figure 8b. (The $NaNO_3$ byproduct is also shown in Figure 8b.) The sodium cations in $Ca_{0.67}Na_{0.67}Eu_{1.33}La_{0.67}Ti_3O_{10}$ are then leached out in acid to form $Ca_{0.67}H_{0.67}Eu_{1.33}La_{0.67}Ti_3O_{10}$ [tetragonal, $a = 7.5727(9)$, $c = 27.621(3)$], which is shown in Figure 8c. Both of these ion-exchanged phases appear from XRD analysis to be single-phase materials, and the lattice constants change only slightly to reflect

the different sizes of the interlayer cations. Likewise, EDS analysis indicates a Ca:Eu ratio of 0.71:1.33 in $Ca_{0.67}H_{0.67}Eu_{1.33}La_{0.67}Ti_3O_{10}$, which is consistent with the expected stoichiometry, within experimental error.

When heated in flowing hydrogen for 1 h at 750 °C, $Ca_{0.67}H_{0.67}Eu_{1.33}La_{0.67}Ti_3O_{10}$ forms $Ca_{0.67}Eu_{1.33}La_{0.67}$-$Ti_3O_9$ (Figure 8d), which is an $SrTiO_3$-type cubic perovskite. All of the major peaks index to a single cubic phase with $a = 3.8825(4)$, which is slightly smaller than $EuTiO_3$ ($a = 3.905$)[102] and reflects the incorporation of La^{3+} and Ca^{2+}, which are smaller than Eu^{2+}, into the A-sites of the product perovskite. (A few broad, low-intensity peaks in the XRD pattern of $CaEu_{1.33}La_{0.67}$-Ti_3O_9 are consistent with the unexchanged parent phase $Na_2Eu_{1.33}La_{0.67}Ti_3O_{10}$, which reduces but does not collapse. Similar results were obtained in the $AEu_2Ti_3O_9$ system reported previously.[40]) The absence of a low-angle reflection at ca. $3a$, or 7.6° 2θ, indicates that Ca^{2+}, Eu^{2+}, and La^{3+} are disordered among the A-sites of the perovskite lattice, which is reasonable considering both the temperature of the reaction and the availability of vacant A-sites.
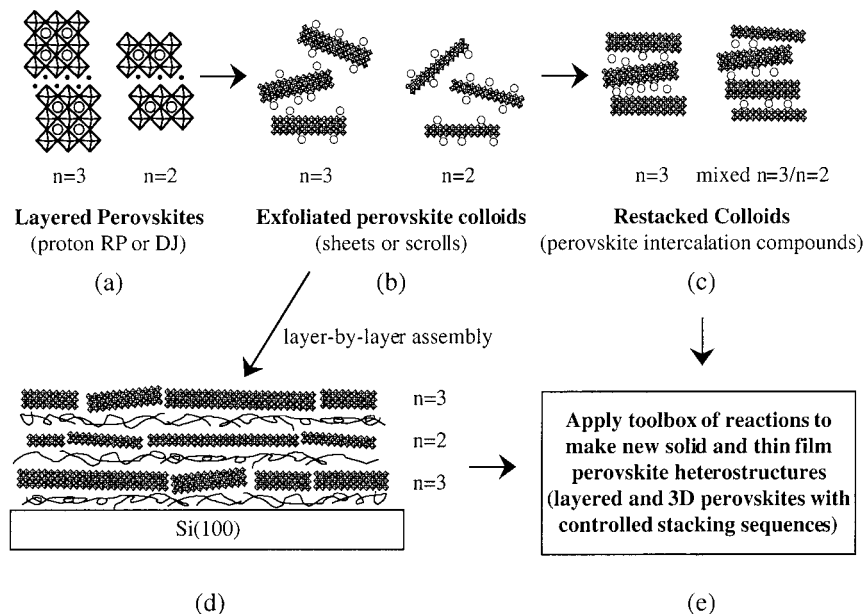
Figure 9. Exfoliation and layer-by-layer assembly of thin-film layered perovskite heterostructures.

By combining topochemical dehydration and reduction, we were able to synthesize a new perovskite containing an intermediate number of A-site defects, and this approach could be extended to include other members of the $Ca_{x/2}Eu_xLa_{2-x}Ti_3O_9$ series as well as other related phases. Using this approach, it is possible to precisely define the number of defect sites in the product perovskite simply by adjusting the ratio of Eu:La in the layered precursor and the amount of Ca^{2+} that is exchanged for Na^+ in the ion-exchange step. By applying this approach to layered perovskite precursors that contain reducible B-site cations, such as $Na_2La_2Ti_{3-x}Ru_xO_{10}$[94] and $Na_2Ln_2Ti_{3-x}Mn_xO_{10}$,[50] it may be possible to fine-tune the oxidation state of Ru or Mn in the product perovskite phase by using substoichiometric ion exchange followed by combined topochemical dehydration and reduction. Work along these lines is currently in progress.

Extending the Toolbox—Layer-by-Layer Assembly of Thin-Film Layered Perovskites

Most of the reactions in the toolbox begin with layered perovskite precursors, and the reactions transform them into new layered or three-dimensional phases. These reactions are powerful, but they are somewhat limited by the perovskite-block stacking sequences that are accessible in the layered precursors, which are synthesized at high temperatures. For example, the A-site cations in $CaEu_2Ti_3O_9$ are ordered and can be modified in the ion-exchange step,[40] but the perovskite block stacking sequence is constrained to the $EuTiO_3$-type unit that is present in the precursor phase. Using this solid-state approach, more complex stacking sequences, such as intergrowths of titanate and manganate octahedra in alternating triple-layer perovskite blocks, are impossible to synthesize unless they can be formed initially in the precursor phase.

An alternate approach for synthesizing new perovskites with complex "made-to-order" stacking sequences is to exploit the exfoliation and layer-by-layer restacking of layered perovskites as thin films. Upon reaction with

a bulky organic base such as tetra-(n-butyl)ammonium hydroxide (TBA^+OH^-), the proton forms of many layered perovskites exfoliate into colloidal sheets (Figure 9b).[43,62−64] For example, the triple-layer Dion−Jacobson phase $HCa_2Nb_3O_{10}$ exfoliates into $TBA_xH_{1-x}Ca_2Nb_3O_{10}$ sheets, shown in Figure 10a, upon reaction with TBA^+OH^-.[63,64] Other Dion−Jacobson phases, including $HSr_2Nb_3O_{10}$, $HCaLaNb_2TiO_{10}$, $HLa_2Ti_2NbO_{10}$, and $H-LaNb_2O_7$,[64] and some Ruddlesden−Popper phases, including $H_2SrLaTi_2TaO_{10}$ and $H_2Ca_2Ta_2TiO_{10}$,[62] behave similarly.

In some cases, the exfoliation conditions can modify the morphology of the nanoscale colloids. For example, when reacted with TBA^+OH^- for several days at room temperature, the Ruddlesden−Popper phase $H_2CaNa-Ta_3O_{10}$ forms a mixture of colloidal sheets and scrolls.[62] By changing the reaction temperature to 35 °C, the colloids cleave to form the nanoscale fibers shown in Figure 10b. The Ruddlesden−Popper phase $H_2La_2Ti_3O_{10}$ can also adopt a variety of morphologies, depending on the exfoliant. When exfoliated with TBA^+OH^- or n-butylamine, colloidal sheets similar to those of $HCa_2-Nb_3O_{10}$ are formed.[62] When exfoliated with a polymeric surfactant, nearly monodisperse 100 × 20 nm scrolls are formed (Figure 10c).[62]

Colloidal sheets made in this way are negatively charged, and they can be self-assembled into monolayer thin films on cationic substrates (Figure 9d).[62−64] For example, $TBA_xH_{1-x}Ca_2Nb_3O_{10}$ can be self-assembled into a tiled monolayer of sheets on an oxidized Si(110) surface that has been derivatized with the cationic polymer poly(diallyldimethylammonium chloride) (PD-DA).[64] Because the thin-film growth method is electrostatic, deposition stops at monolayer coverage when all of the positive charge has been compensated by the negative charge of the sheets.[103] Subsequently, PDDA can be adsorbed on top of the negatively charged sheets, which again renders the surface positively charged to allow further deposition of sheets.

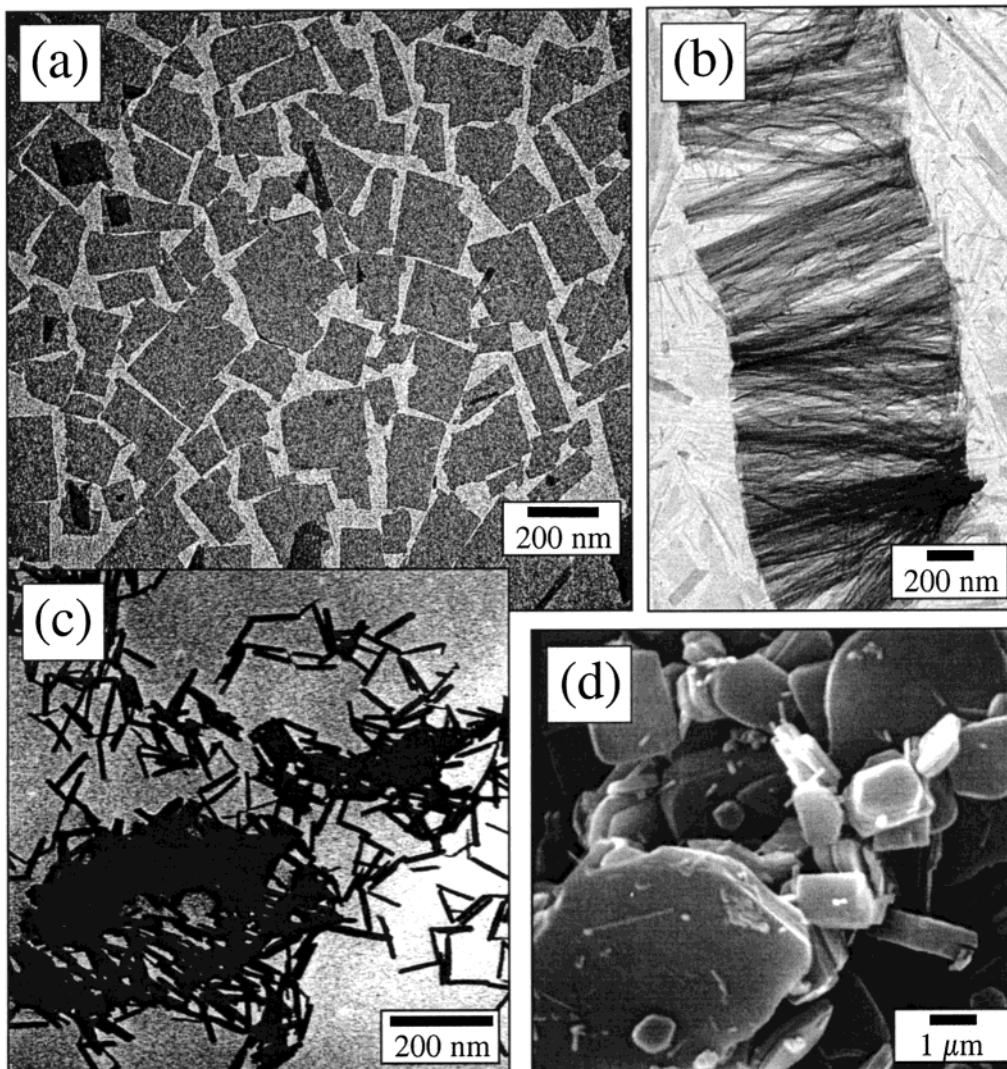When this layer-by-layer process is used, any desired stacking sequence can be assembled as a thin film.

Figure 10. Transmission electron micrographs of (a) colloidal $TBA_xH_{1-x}Ca_2Nb_3O_{10}$ sheets, (b) $TBA_xH_{2-x}CaNaTa_3O_{10}$ fibers formed by reacting $H_2CaNaTa_3O_{10}$ with TBA^+OH^- at 35 °C, and (c) monodisperse scrolls of $H_2La_2Ti_3O_{10}$ exfoliated with a polymeric amine surfactant. A scanning electron micrograph of the A-site ordered perovskite $CaEu_2Ti_3O_9$ synthesized by topochemical reduction of $CaEu_2Ti_3O_{10}$ is shown in (d) to highlight the anisotropic morphology of the microcrystallites.

Thus, we have succeeded in making a layered perovskite thin film of $PDDA_xH_{1-x}(Ca,Sr)Nb_3O_{10}$, which is a polymer intercalation compound of $HCa_2Nb_3O_{10}$ and $HSr_2Nb_3O_{10}$ with the Ca^{2+} and Sr^{2+} cations ordered in successive triple-layer perovskite blocks.[64] Likewise, the more complex stacking sequence $HCa_2Nb_3O_{10}/HLaNb_2O_7/HSr_2Nb_3O_{10}/HLaNb_2O_7$ (interleaved with PDDA) was easily synthesized using layer-by-layer assembly.[64] This thin-film sequence represents an intergrowth of the Dion–Jacobson phases $HA_2Nb_3O_{10}$ (A = Ca, Sr) and $HLaNb_2O_7$, where the Ca^{2+} and Sr^{2+} cations are ordered in successive layers of the triple-layer perovskite blocks, which themselves are separated by double-layer $[LaNb_2O_7]^-$ blocks. Such complex stacking sequences are impossible to synthesize using traditional high-temperature methods.

By exploiting the layer-by-layer assembly of perovskite thin films, it is possible to synthesize layered perovskites that contain complex stacking sequences. Thus, applying the toolbox of solid-state reactions to the thin-film heterostructures would be a powerful approach for dramatically expanding the number of new perovskite phases that can be synthesized retrosynthetically

(Figure 9e). The thin-film layered perovskites, which have a polycation between the layers, can be converted to their proton forms by burning off the organic materials between the layers.[63] Using the toolbox of reactions, one could begin converting these thin films into other layered or three-dimensional perovskites. While the thin films are well-ordered along the stacking axis, they are randomly aligned in the plane of the perovskite sheets, so subsequent topochemical reactions will be limited to the formation of disordered polycrystalline films. Several approaches for orienting these sheets epitaxially on a surface are under study to greatly improve the quality of the self-assembled thin films.

As a bulk-phase alternative to layer-by-layer assembly, it is also possible to restack exfoliated perovskite colloids by flocculating them with a variety of ion-exchange media (Figure 9c). For example, acid treatment of $TBA_xH_{1-x}Ca_2Nb_3O_{10}$[63] or $(ACA)Ca_2Nb_3O_{10}$[65] immediately yields $HCa_2Nb_3O_{10}$, although as in the thin films there is significant orientational disorder in the plane of the perovskite sheets. $TBA_xH_{1-x}Ca_2Nb_3O_{10}$ and related phases can also be restacked with a variety of mono-, di-, and trivalent cations.[104] Interestingly, we

recently found that upon reaction of $TBA_xH_{1-x}Ca_2Nb_3O_{10}$ or $TBA_xH_{1-x}LaNb_2O_7$ with cetyltrimethylammonium bromide (CTAB), the highly charged trimethylammonium group of CTAB displaces the weakly bound TBA^+ cations,[104] resulting in a bulk-phase intercalation solid that has a bilayer arrangement of the alkyl chains as in $n\text{-}C_8H_{17}NH_3[Ca_2Nb_3O_{10}]$.[42] By restacking several types of exfoliated layered perovskites into a single bulk solid, it may be possible to form a variety of intergrowths that could have interesting structures or properties. Likewise, these bulk-phase materials could be useful intermediates to their thin-film analogues, and subsequent topochemical reactions could also yield many new interesting perovskite phases. Because both Ruddlesden−Popper and Dion−Jacobson phases are amenable to layer-by-layer assembly and because Aurivillius phases can be converted into Ruddlesden−Popper solid acids,[61] one could in principle synthesize a rich variety of new perovskites as thin films or bulk solids by controlled restacking and layer-by-layer assembly.

Conclusions and Future Directions

In this review, we have proposed and demonstrated the concept of retrosynthetic design using low-temperature reactions of layered perovskites. The individual reactions can be classified into sets involving ion exchange of discrete interlayer cations, ion exchange of cationic interlayer structural units, condensation of interlayer oxide ligands, and other transformations that involve high-pressure or low-temperature intercalation/deintercalation processes. When all of these reactions are combined, a powerful toolbox of solid-state reactions emerges, and it is possible to rationally synthesize a variety of new layered and three-dimensional perovskites as solids and thin films.

While we have shown many reactions and numerous examples of solid-state retrosynthesis, the toolbox is not yet complete, and its full potential has not yet been realized. In fact, research into the rational synthesis of new perovskites is just beginning, and several important challenges remain. First, the product perovskites retain the structural features of the layered precursors, which means that synthesizing the appropriate precursors is of primary importance. Although new examples frequently appear in the literature, there are still only a limited number of ion-exchangeable Ruddlesden−Popper and Dion−Jacobson titanates, niobates, and tantalates, and only a small number of Aurivillius phases have been converted into ion-exchangeable layered perovskites. Likewise, incorporating electronically and magnetically interesting cations into the A- and B-sites of ion-exchangeable layered perovskites remains a challenge, and to date the maximum doping level remains at one-third of the B-site cations, as in $Na_2Sr_2Nb_2MnO_{10}$, $Na_2La_2Ti_2RuO_{10}$,[94] $Na_2Ln_2Ti_2MnO_{10}$,[50] and $CsLaSrNb_2CuO_9$.[36] Synthetic efforts are needed to extend the level of doping as well as to explore other interesting cations and structural features such as B-site or A-site cation ordering within the perovskite block. Likewise, detailed characterization is necessary to fully understand the structures of the product perovskites because disorder is inherent in these materials. Once these synthetic and characterization challenges are met, a wider range of perovskites can be synthesized by design.

Another important challenge is to fully exploit the rational design of perovskites to target the development of new phases that have interesting and useful properties. Many of the interesting product phases contain mixed-valent B-site cations, including the $Cu^{2+/3+}$ superconductors and the $Mn^{3+/4+}$ magneoresistive materials. By combining reactions such as ion exchange and topochemical condensation, it may be possible to retrosynthetically program the final oxidation state in a product perovskite, much like Wiley and co-workers have done for $Na_{1-x+y}Ca_{x/2}LaTiO_4$.[71] Likewise, these rational approaches to property design could be extended to allow solid-state chemists to study structure/relationships in similar phases. For instance, by carefully controlling the oxidation state of a product phase by ion exchange or topochemical condensation, one could monitor subtle changes in structure and properties, such as magnetic susceptibility or electrical conductivity, as a function of oxidation state in a homologous series of phases. In addition, layered perovskites have highly anisotropic crystallites and the topochemical transformations retain this morphology (Figure 10d), so it may be possible to design highly textured cubic phases that are magnetic or ferroic.

Finally, the reactions reported up to this point are not exhaustive, and there are many additional reactions that one could envision for synthesizing new types of layered perovskites and for targeting new structural features in three-dimensional perovskites. For example, Gopalakrishnan and co-workers synthesized layered perovskites with intermediate interlayer charges that bridge the Ruddlesden−Popper and Dion−Jacobson series,[60] and a related series has a layer charge that varies from 0 to $+1$.[105] Developing reactions for these phases with intermediate interlayer charge densities could provide access to new intergrowth structures or allow even more control over A-site defect concentration and oxidation state. Reactions that focus on the anions in the perovskite structure could also be important for controlling properties and structural features because, for example, superconductivity in cuprates can be enhanced by the substitution of oxygen for fluorine.[87] Such reactions could exploit new precursor phases such as the ion-exchangeable Dion−Jacobson oxyfluorides $ASrNb_2O_6F$ (A = Li, Na, Rb)[106] and the Ruddlesden−Popper oxysulfides $Ln_2Ti_2S_2O_5$ (Ln = Nd, Pr, Sm).[107] Developing analogous reactions for non-oxide perovskite phases, such as the metal/organic layered perovskites,[32] the pnictide-oxide K_2NiF_4-type structures,[108] and the superconducting intermetallic phases,[33] could further extend the scope and applicability of the toolbox and allow one to target important properties and structural features using the ideas of solid-state inorganic retrosynthesis.

References

(1) Cheetham, A. K.; Day, P. In *Solid State Chemistry: Techniques*; Clarendon Press: Oxford, 1987.
(2) Rao, C. N. R.; Gopalakrishnan, J. In *New Directions in Solid State Chemistry*, 2nd ed.; Cambridge University Press: Cambridge, 1997.

(3) Feng, S.; Xu, R. *Acc. Chem. Res.* **2001**, *34*, 239.
(4) (a) Livage, J.; Henry, M.; Sanchez, C. *Prog. Solid State Chem.* **1988**, *18*, 259. (b) Jolivet, J.-P. In *Metal Oxide Chemistry and Synthesis: From Solution to Solid State*; John Wiley: New York, 2000.
(5) (a) Braga, D.; Grepioni, F.; Desiraju, G. R. *Chem. Rev.* **1998**, *98*, 1375. (b) Caulder, D. L.; Raymond, K. N. *Acc. Chem. Res.* **1999**, *32*, 975. (c) Braga, D.; Grepioni, F. *Acc. Chem. Res.* **2000**, *33*, 601. (d) Plaut, D. J.; Holman, K. T.; Pivovar, A. M.; Ward, M. D. *J. Phys. Org. Chem.* **2000**, *13*, 858. (e) Moulton, B.; Zaworotko, M. J. *Chem. Rev.* **2001**, *101*, 1629.
(6) (a) Li, H. L.; Laine, A.; O'Keeffe, M.; Yaghi, O. M. *Science* **1999**, *283*, 1145. (b) Rao, C. N. R.; Natarajan, S.; Neeraj, S. *J. Am. Chem. Soc.* **2000**, *122*, 2810. (c) Zhu, J.; Bu, X.; Feng, P.; Stucky, G. D. *J. Am. Chem. Soc.* **2000**, *122*, 11563. (d) Rao, C. N. R.; Natarajan, S.; Choudhury, A.; Neeraj, S.; Ayi, A. A. *Acc. Chem. Res.* **2001**, *34*, 80.
(7) (a) Yaghi, O. M.; Li, H.; Groy, T. L. *J. Am. Chem. Soc.* **1996**, *118*, 9096. (b) Yaghi, O. M.; Li, H.; Davis, C.; Richardson, D.; Groy, T. L. *Acc. Chem. Res.* **1998**, *31*, 474. (c) Li, H.; Eddaoudi, M.; O'Keeffe, M.; Yaghi, O. M. *Nature* **1999**, *402*, 276. (d) Barton, T. J.; Bull, L. M.; Klemperer, W. G.; Loy, D. A.; McEnaney, B.; Misono, M.; Monson, P. A.; Pez, G.; Scherer, G. W.; Vartuli, J. C.; Yaghi, O. M. *Chem. Mater.* **1999**, *11*, 2633. (e) Eddaoudi, M.; Li, H.; Yaghi, O. M. *J. Am. Chem. Soc.* **2000**, *122*, 1391. (f) Kepert, C. J.; Prior, T. J.; Rosseinsky, M. J. *J. Am. Chem. Soc.* **2000**, *122*, 5158. (g) Eddaoudi, M.; Kim, J.; Wachter, J. B.; Chae, H. K.; O'Keeffe, M.; Yaghi, O. M. *J. Am. Chem. Soc.* **2001**, *123*, 4368. (h) Chen, B. L.; Eddaoudi, M.; Hyde, S. T.; O'Keeffe, M.; Yaghi, O. M. *Science* **2001**, *291*, 1021.
(8) (a) O'Keeffe, M.; Eddaoudi, M.; Li, H. L.; Reineke, T.; Yaghi, O. M. *J. Solid State Chem.* **2000**, *152*, 3. (b) Ferey, G. *J. Solid State Chem.* **2000**, *152*, 37. (c) Eddaoudi, M.; Moler, D. B.; Li, H.; Chen. B.; Reineke, T. M.; O'Keeffe, M.; Yaghi, O. M. *Acc. Chem. Res.* **2001**, *34*, 319.
(9) (a) Long, J. R.; McCarty, L. S.; Holm, R. H. *J. Am. Chem. Soc.* **1996**, *118*, 4603. (b) Henry, M. *Coord. Chem. Rev.* **1998**, *180*, 1109. (c) Axtell, E. A.; Park, Y.; Chondroudis, K.; Kanatzidis, M. G. *J. Am. Chem. Soc.* **1998**, *120*, 124. (d) Tulsky, E. G.; Long, J. R. *Chem. Mater.* **2001**, *13*, 1149.
(10) (a) Theis, D.; Yeh, J.; Schlom, D. G.; Hawley, M. E.; Brown, G. W.; Jiang, J. C.; Pan, X. Q. *Appl. Phys. Lett.* **1998**, *72*, 2817. (b) Lettieri, J.; Jia, Y.; Urbanik, M.; Weber, C. I.; Maria, J.-P.; Schlom, D. G.; Li, H.; Ramesh, R.; Uecker, R.; Reiche, P. *Appl. Phys. Lett.* **1998**, *73*, 2923. (c) Haeni, J. H.; Theis, C. D.; Schlom, D. G.; Tian, W.; Pan, X. Q.; Chang, H.; Takeuchi, I.; Xiang, X. D. *Appl. Phys. Lett.* **2001**, *78*, 3292.
(11) Lowndes, D. H.; Geohegan, D. B.; Puretzky, A. A.; Norton, D. P.; Rouleau, C. M. *Science* **1996**, *273*, 898.
(12) Switzer, J. A.; Shumsky, M. G.; Bohannan, E. W. *Science* **1999**, *284*, 293.
(13) (a) Novet, T.; Johnson, D. C. *J. Am. Chem. Soc.* **1991**, *113*, 3398. (b) Novet, T.; McConnell, J. M.; Johnson, D. C. *Chem. Mater.* **1992**, *4*, 473. (c) Fister, L.; Johnson, D. C. *J. Am. Chem. Soc.* **1992**, *114*, 4639. (d) Xu, Z.; Tang, Z.; Devan, S. D.; Novet, T.; Johnson, D. C. *J. Appl. Phys.* **1993**, *74*, 905. (e) Sellinschegg, H.; Stuckmeyer, S. L.; Hornbostsel, M. D.; Johnson, D. C. *Chem. Mater.* **1998**, *10*, 1096. (f) Schneidmiller, R.; Bentley, A.; Hornbostel, M. D.; Johnson, D. C. *J. Am. Chem. Soc.* **1999**, *121*, 3142. (g) Hughes, T. A.; Kevan, S. D.; Cox, D. E.; Johnson, D. C. *J. Am. Chem. Soc.* **2000**, *122*, 8910. (h) Williams, J. R.; Johnson, M.; Johnson, D. C. *J. Am. Chem. Soc.* **2001**, *123*, 1645.
(14) For example, see (a) Tournoux, M.; Marchand, R.; Brohan, L. *Prog. Inorg. Solid State Chem.* **1986**, *17*, 33. (b) Figlarz, M. *Chem. Scr.* **1988**, *28*, 3. (c) Figlarz, M.; Gérand, B.; Delahaye-Vidal, A.; Dumont, B.; Harb, F.; Coucou, A.; Fievet, F. *Solid State Ionics* **190**, *43*, 143. (d) Figlarz, M.; Gerand, B.; Dumont, B.; Delahayevidal, A.; Portemer, F. *Phase Transitions* **1991**, *31*, 167. (e) Stein, A.; Keller, S. W.; Mallouk, T. E. *Science* **1993**, *259*, 1558. (f) Schleich, D. M. *Solid State Ionics* **1994**, *70*, 407. (g) Gopalakrishnan, J. *Chem. Mater.* **1995**, *7*, 1265. (h) Rouxel, J.; Tournoux, M. *Solid State Ionics* **1996**, *84*, 141.
(15) Galasso, F. S. *Structure, Properties and Preparation of Perovskite-type Compounds*; Pergamon Press: Oxford, 1969.
(16) Dion, M.; Ganne, M.; Tournoux, M. *Mater. Res. Bull.* **1981**, *16*, 1429.
(17) Dion, M.; Ganne, M.; Tournoux, M.; Revez, J. *Rev. Chim. Miner.* **1984**, *21*, 92.
(18) (a) Ruddlesden, S. N.; Popper, P. *Acta Crystallogr.* **1957**, *10*, 538; *Acta Crystallogr.* **1958**, *11*, 54.
(19) (a) Gopalakrishnan, J.; Bhat, V. *Inorg. Chem.* **1987**, *26*, 4301.
(20) (a) Aurivillius, B. *Ark. Kemi* **1949**, *1*, 463. (b) Aurivillius, B. *Ark. Kemi* **1949**, *1*, 499.
(21) For example, see (a) Bednorz, J. G.; Müller, K. A. *Z. Phys. B* **1986**, *64*, 189. (b) Schneemeyer, L. F.; Waszczak, J. V.; Siegrist, T.; Vandover, R. B.; Rupp, L. W.; Batlogg, B.; Cava, R. J.; Murphy, D. W. *Nature* **1987**, *328*, 601. (c) Cava, R. J.; Batlogg, B.; Krajewski, J. J.; Rupp, L. W.; Schneemeyer, L. F.; Siegrist, T.; Vandover, R. B.; Marsh, P.; Peck, W. F.; Gallagher, P. K.;

Glarum, S. H.; Marshall, J. H.; Farrow, R. C.; Waszczak, J. V.; Hull, R.; Trevor, P. *Nature* **1988**, *336*, 211. (d) Cava, R. J.; Batlogg, B.; Krajewski, J. J.; Farrow, R.; Rupp, L. W.; Rupp, L. W.; White, A. E.; Short, K.; Peck, W. F.; Kometani, T. *Nature* **1988**, *332*, 814. (e) Cava, R. J. *Sci. Am.* **1990**, *263*, 42. (f) Cava, R. J. *J. Am. Ceram. Soc.* **2000**, *83*, 5.
(22) For example, see (a) Jin, S.; Tiefel, T. H.; McCormack, M.; Fastnacht, R. A.; Ramesh, R.; Chen, L. H. *Science* **1994**, *264*, 315. (b) Rao, C. N. R.; Cheetham, A. K.; Mahesh, R. *Chem. Mater.* **1996**, *8*, 2421. (c) Kuwahara, H.; Tomioka, Y.; Moritomo, Y.; Asamitsu, A.; Kasai, M.; Kumai, R.; Tokura, Y. *Science* **1996**, *272*, 80. (d) Kimura, T.; Tomioka, Y.; Kuwahara, H.; Asamitsu, A.; Tamura, M.; Tokura, Y. *Science* **1996**, *274*, 1698. (e) Maignan, A.; Martin, C.; Damay, F.; Raveau, B. *Chem. Mater.* **1998**, *10*, 950. (f) Raveau, B.; Maignan, A.; Martin, C.; Hervieu, M. *Chem. Mater.* **1998**, *10*, 2641. (g) Kobayashi, K. L.; Kimura, T.; Sawada, H.; Terakura, K.; Tokura, Y. *Nature* **1998**, *395*, 677.
(23) Moritomo, Y.; Asamitsu, A.; Kuwahara, H.; Tokura, Y. *Nature* **1996**, *380*, 141.
(24) For example, see (a) Brahmaroutu, B.; Messing, G. L.; Trolier-McKinstry, S.; Selvaraj, U. In *Proceedings of the 10th IEEE International Symposium on Applications of Ferroelectrics, Vol II*; Kulwicki, B. M., Amin, A., Safari, A., Eds.; IEEE: Piscataway, NJ, 1996; pp 883−886. (b) Seabaugh, M.; Hong, S.-H.; Messing, G. L. In *Ceramic Microstructure: Control at the Atomic Level*; Tomsia, A. P.; Glaeser, A., Eds.; Plenum Press: New York, 1998; pp 303−310. (c) Takeuchi, T.; Tani, T.; Satoh, T. *Solid State Ionics* **1998**, *108*, 67. (d) Tani, T. *J. Korean Phys. Soc.* **1998**, *32*, S1217. (e) Horn, J.; Zhang, S. C.; Selvaraj, U.; Messing, G. L.; Trolier-McKinstry, S. *J. Am. Ceram. Soc.* **1999**, *82*, 921. (f) Rehrig, P. W.; Park, S.-E.; Trolier-McKinstry, S.; Messing, G. L.; Jones, B.; Shrout, T. R. *J. Appl. Phys.* **1999**, *86*, 1657.
(25) Peña, M. A.; Fierro, J. L. G. *Chem. Rev.* **2001**, *101*, 1981.
(26) (a) Otzschi, K. D.; Poeppelmeier, K. R.; Salvador, P. A.; Mason, T. O.; Zhang, H.; Marks, L. D. *J. Am. Chem. Soc.* **1996**, *118*, 8951. (b) Salvador, P. A.; Greenwod, K. B.; Mawdsley, J. R.; Poeppelmeier, K. R.; Mason, T. O. *Chem. Mater.* **1999**, *11*, 1760.
(27) (a) Takata, M.; Furumi, Y.; Shinohara, K.; Tanaka, A.; Hara, M.; Kondo, J. N.; Domen, K. *Chem. Mater.* **1997**, *9*, 1063. (b) Machida, M.; Yabunaka, J.; Kijima, T. *Chem. Mater.* **2000**, *12*, 812.
(28) Rebbah, H.; Desgardin, G.; Raveau, B. *Mater. Res. Bull.* **1979**, *14*, 1125.
(29) (a) Marchand, R.; Brohan, L.; Tournoux, M. *Mater. Res. Bull.* **1980**, *15*, 1129. (b) Feist, T. P.; Mocarski, S. J.; Davies, P. K.; Jacobson, A. J.; Lewandowski, J. T. *Solid State Ionics* **1988**, *28−30*, 1338. (c) Feist, T. P.; Davies, P. K. *J. Solid State Chem.* **1992**, *101*, 275.
(30) (a) Figlarz, M. *Prog. Solid State Chem.* **1989**, *19*, 1. (b) McCarron, E. M. *J. Chem. Soc., Chem. Commun.* **1986**, 336.
(31) Iordanidis, L.; Kanatzidis, M. G. *J. Am. Chem. Soc.* **2000**, *122*, 8319.
(32) (a) Wang, S.; Mitzi, D. B.; Landrum, G. A.; Genin, H.; Hoffmann, R. *J. Am. Chem. Soc.* **1997**, *119*, 724. (b) Kagan, C. R.; Mitzi, D. B.; Dimitrakopoulos, C. D. *Science* **1999**, *286*, 945. (c) Chondrousid, K.; Mitzi, D. B. *Chem. Mater.* **1999**, *11*, 3028. (d) Mitzi, D. B.; Chondroudis, K.; Kagan, C. R. *Inorg. Chem.* **1999**, *38*, 6246. (e) Mitzi, D. B.; Dimitrakopoulos, C. D.; Kosbar, L. L. *Chem. Mater.* **2001**, *13*, 3728.
(33) He, T.; Huang, Q.; Ramirez, A. P.; Wang, T.; Regan, K. A.; Rogado, N.; Hayward, M. A.; Haas, M. K.; Slusky, J. S.; Inumaru, H. W.; Zandbergen, H. W.; Cava, R. J. *Nature* **2001**, *411*, 54.
(34) (a) Sato, M.; Abo, J.; Jin, T. *Solid State Ionics* **1992**, *57*, 285. (b) Toda, K.; Sato, M. *J. Mater. Chem.* **1996**, *6*, 1067.
(35) Gopalakrishnan, J.; Uma, S.; Bhat, V. *Chem. Mater.* **1993**, *5*, 132.
(36) Gopalakrishnan, J.; Uma, S.; Vasanthacharya, N. Y.; Subbanna, G. N. *J. Am. Chem. Soc.* **1995**, *117*, 2353.
(37) (a) Thangadurai, V.; Shukla, A. K.; Gopalakrishnan, J. *Solid State Ionics* **1994**, *73*, 9. (b) Byeon, S.-H.; Park, K.; Itoh, M. *J. Solid State Chem.* **1996**, *121*, 430. (c) Thangadurai, V.; Weppner, W. *J. Mater. Chem.* **2001**, *11*, 636.
(38) (a) Toda, K.; Kurita, S.; Sato, M. *J. Ceram. Soc. Jpn.* **1996**, *104*, 140. (b) Thangadurai, V.; Shukla, A. K.; Gopalakrishnan, J.; Joubert, O.; Brohan, L.; Tournoux, M. *Mater. Sci. Forum* **2000**, *321−323*, 965.
(39) (a) Blasse, G. *J. Inorg. Nucl. Chem.* **1968**, *30*, 656. (b) Toda, K.; Kameo, Y.; Kurita, S.; Sato, M. *J. Alloys Cmpds.* **1996**, *234*, 19. (c) Byeon, S.-H.; Park, K. *J. Solid State Chem.* **1996**, *121*, 430.
(40) Schaak, R. E.; Mallouk, T. E. *J. Am. Chem. Soc.* **2000**, *122*, 2798.
(41) (a) Mahler, C. H.; Cushing, B. L.; Lalena, J. N.; Wiley, J. B. *Mater. Res. Bull.* **1998**, *33*, 1581. (b) Cushing, B. L.; Wiley, J. B. *Mater. Res. Bull.* **1999**, *34*, 271.
(42) Jacobson, A. J.; Johnson, J. W.; Lewandowski, J. T. *Inorg. Chem.* **1985**, *24*, 3729.
(43) Treacy, M. M. J.; Rice, S. B.; Jacobson, A. J.; Lewandowski, J. T. *Chem. Mater.* **1990**, *2*, 279.
(44) Uma, S.; Gopalakrishnan, J. *Chem. Mater.* **1994**, *6*, 907.

Reviews

Chem. Mater., Vol. 14, No. 4, 2002 **1471**

(45) For example, see (a) Lagaly, G. *Solid State Ionics* **1986**, *22*, 43. (b) Kinomura, N.; Kumada, N. *Solid State Ionics* **1992**, *51*, 1. (c) Bhuvanesh, N. S. P.; Gopalakrishnan, J. *Inorg. Chem.* **1995**, *34*, 3760.

(46) Hong, Y. S.; Kim, S. J.; Kim, S. J.; Choy, J. H. *J. Mater. Chem.* **2000**, *10*, 1209.

(47) (a) Matsuda, T.; Miyamae, N.; Takeuchi, M. *Bull. Chem. Soc. Jpn.* **1993**, *66*, 1551. (b) Takahashi, S.; Nakato, T.; Hayashi, S.; Sugahara, Y.; Kuroda, K. *Inorg. Chem.* **1995**, *34*, 5065.

(48) (a) Hong, Y. S.; Kim, K. *Chem. Lett.* **2000**, *6*, 690. (b) Hong, Y. S.; Han, C. H.; Kim, K. *J. Solid State Chem.* **2001**, *158*, 290. (c) Hong, Y. S.; Kim, K. *Mater. Res. Bull.* **2001**, *36*, 1325.

(49) (a) Toda, K.; Watanabe, J.; Sato, M. *Solid State Ionics* **1996**, *90*, 15. (b) Toda, K.; Watanabe, J.; Sato, M. *Mater. Res. Bull.* **1996**, *31*, 1427.

(50) Schaak, R. E.; Afzal, D.; Mallouk, T. E., *Chem. Mater.* **2002**, *14*, 442.

(51) Hyeon, K.; Byeon, S. *Chem. Mater.* **1999**, *11*, 352.

(52) Gopalakrishnan, J.; Sivakumar, T.; Ramesha, K.; Thangadurai, V.; Subbanna, G. N. *J. Am. Chem. Soc.* **2000**, *122*, 6237.

(53) Ollivier, P. J.; Mallouk, T. E. *Chem. Mater.* **1998**, *10*, 2585.

(54) Schaak, R. E.; Mallouk, T. E. *J. Solid State Chem.* **2000**, *155*, 46.

(55) Richard, M.; Brohan, L.; Tournoux, M. *J. Solid State Chem.* **1994**, *112*, 345.

(56) Bhuvanesh, N. S. P.; Crosnier-Lopez, M. P.; Duroy, H.; Fourquet, J. L. *J. Mater. Chem.* **2000**, *10*, 1685.

(57) Schaak, R. E.; Mallouk, T. E. *J. Solid State Chem.* **2001**, *161*, 225.

(58) Schaak, R. E.; Mallouk, T. E., unpublished results.

(59) Jacobson, A. J.; Lewandowski, J. T.; Johnson, J. W. *Mater. Res. Bull.* **1990**, *25*, 679.

(60) Uma, S.; Raju, A. R.; Gopalakrishnan, J. *J. Mater. Chem.* **1993**, *3*, 709.

(61) (a) Sugimoto, W.; Shirata, M.; Sugahara, Y.; Kuroda, K. *J. Am. Chem. Soc.* **1999**, *121*, 11601. (b) Shirata, M.; Tsunoda, Y.; Sugimoto, W.; Sugahara, Y. *Mater. Res. Soc. Symp. Proc.* **2002**, *658*, in press.

(62) Schaak, R. E.; Mallouk, T. E. *Chem. Mater.* **2000**, *12*, 3427.

(63) Fang, M.; Kim, H.-N.; Saupe, G. B.; Miwa, T.; Fujishima, A.; Mallouk, T. E. *Chem. Mater.* **1999**, *11*, 1526.

(64) Schaak, R. E.; Mallouk, T. E. *Chem. Mater.* **2000**, *12*, 2513.

(65) Han, Y.-S.; Park, I.; Choy, J.-H. *J. Mater. Chem.* **2001**, *11*, 1277.

(66) Armstrong, A. R.; Anderson, P. A. *Inorg. Chem.* **1994**, *33*, 4366.

(67) (a) Toda, K.; Teranishi, T.; Takahashi, M.; Ye, Z. G.; Sato, M. *Solid State Ionics* **1998**, *115*, 501. (b) Toda, K.; Takahashi, M.; Teranishi, T.; Ye, Z. G.; Sato, M.; Hinatsu, Y. *J. Mater. Chem.* **1999**, *9*, 799. (c) Toda, K.; Teranishi, T.; Ye, Z. G.; Sato, M.; Hinatsu, Y. *Mater. Res. Bull.* **1999**, *34*, 1815.

(68) Choy, J.-H.; Kim, J.-Y.; Chung, I. *J. Phys. Chem. B* **2001**, *105*, 7908.

(69) Toda, K.; Teranishi, T.; Sato, M. *J. Eur. Ceram. Soc.* **1999**, *19*, 1525.

(70) Fukuoka, H.; Isami, T.; Yamanaka, S. *Chem. Lett.* **1997**, 703.

(71) McIntyre, R. A.; Falster, A. U.; Li, S.; Simmons, W. B., Jr.; O'Connor, C. J.; Wiley, J. B. *J. Am. Chem. Soc.* **1998**, *120*, 217.

(72) Lalena, J. N.; Cushing, B. L.; Falster, A. U.; Simmons, W. B., Jr.; Seip, C. T.; Carpenter, E. E.; O'Connor, C. J.; Wiley, J. B. *Inorg. Chem.* **1998**, *37*, 4484.

(73) Tsunoda, Y.; Shirata, M.; Sugimoto, W.; Liu, Z.; Terasaki, O.; Kuroda, K.; Sugahara, Y. *Inorg. Chem.*, **2001**, *40*, 5768.

(74) Kodenkandath, T. A.; Lalena, J. N.; Zhou, W. L.; Carpenter, E. E.; Sangregorio, C.; Falster, A. U.; Simons, W. B., Jr.; O'Connor, C. J.; Wiley, J. B. *J. Am. Chem. Soc.* **1999**, *121*, 10743.

(75) Kodenkandath, T. A.; Kumbhar, A. S.; Zhou, W. L.; Wiley, J. B. *Inorg. Chem.* **2001**, *40*, 710.

(76) Kodenkandath, T. A.; Viciu, M. L.; Zhang, X.; Sims, J. A.; Gilbert, E. W.; Augrain, F.-X.; Chotard, J.-N.; Caruntu, G. A.; Spinu, L.; Zhou, W. L.; Wiley: J. B. *Mater. Res. Soc. Symp. Proc.* **2002**, *658*, in press.

(77) Dulieu, B.; Bullot, J.; Wery, J.; Richard, M.; Brohan, L. *Phys. Rev. B* **1996**, *53*, 10641.

(78) Schaak, R. E.; Mallouk, T. E., unpublished results.

(79) Fang, M. M.; Kim, C. H.; Mallouk, T. E. *Chem. Mater.* **1999**, *11*, 1519.

(80) Schaak, R. E.; Guidry, E. N.; Mallouk, T. E. *J. Chem. Soc., Chem. Commun.* **2001**, 853.

(81) Thangadurai, V.; Subbanna, G. N.; Gopalakrishnan, J. *J. Chem. Soc., Chem. Commun.* **1998**, 1300.

(82) Byeon, S.; Kim, H.; Yoon, J.; Dong, Y.; Yun, H.; Inaguma, Y.; Itoh, M. *Chem. Mater.* **1998**, *10*, 2317.

(83) Vander Griend, D. A.; Boudin, S.; Poeppelmeier, K. R.; Azuma, M.; Toganoh, H.; Takano, M. *J. Am. Chem. Soc.* **1998**, *120*, 11518.

(84) Hayward, M. A.; Green, M. A.; Rosseinsky, M. J.; Sloan, J. *J. Am. Chem. Soc.* **1999**, *121*, 8843.

(85) Hayward, M. A.; Rosseinsky, M. J. *Chem. Mater.* **2000**, *12*, 2182.

(86) Grenier, J.-C.; Bassat, J.-M.; Doumerc, J.-P.; Etourneau, J.; Fang, Z.; Fournes, L.; Petit, S.; Pouchard, M.; Wattiaux, A. *J. Mater. Chem.* **1999**, *9*, 25.

(87) (a) Almamouri, M.; Edwards, P. P.; Greaves, C.; Slaski, M. *Nature* **1994**, *369*, 382. (b) Francesconi, M. G.; Slater, P. R.; Hodges, J. P.; Greaves, C.; Edwards, P. P.; Al-Mamouri, M.; Slaski, M. *J. Solid State Chem.* **1998**, *135*, 17.

(88) Greaves, C.; Kissick, J. L.; Francesconi, M. G.; Aikens, L. D.; Gillie, L. J. *J. Mater. Chem.* **1999**, *9*, 111.

(89) Aikens, L. D.; Li, R. K.; Greaves, C. *J. Chem. Soc., Chem. Commun.* **2000**, 2129.

(90) Choy, J.-H.; Lee, W.; Hwang, S.-J. *J. Mater. Chem.* **2000**, *19*, 1679.

(91) Choy, J.-H.; Kwon, S.-J.; Park, G.-S. *Science* **1998**, *280*, 1589.

(92) Choy, J.-H.; Kwon, S.-J.; Hwang, S.-J.; Kim, Y.-I.; Lee, W. *J. Mater. Chem.* **1999**, *9*, 129.

(93) (a) Zhang, L.; Manthiram, A. *J. Mater. Chem.* **1996**, *6*, 999. (b) Tsang, C.; Dananjay, A.; Kim, J.; Manthiram, A. *Inorg. Chem.* **1996**, *35*, 504. (c) Manthiram, A.; Zhu, Y. T. *J. Electrochem. Soc.* **1996**, *143*, L143. (d) Tsang, C.; Manthiram, A. *J. Electrochem. Soc.* **1997**, *144*, 520.

(94) Lalena, J. N.; Falster, A. U.; Simmons, W. B.; Carpenter, E. E.; Wiggins, J.; Hariharan, S.; Wiley, J. B. *Chem. Mater.* **2000**, *12*, 2418.

(95) (a) Wolfe, R. W.; Newnham, R. E. *J. Electochem. Soc.* **1969**, *116*, 832. (b) Subbanna, G. N.; Guru Row, T. N.; Rao, C. N. R. *J. Solid State Chem.* **1990**, *86*, 206. (c) Champarnaud-Mesjard, J.-C.; Frit, B.; Watanabe, A. *J. Mater. Chem.* **1999**, *9*, 1319.

(96) Schaak, R. E.; Mallouk, T. E., unpublished results.

(97) Yu, W. J.; Kim, Y. I.; Ha, D. H.; Lee, J. H.; Park, Y. K.; Seong, S.; Hur, N. H. *Solid State Commun.* **1999**, *111*, 705.

(98) $H_2[Sr_2Nb_2MnO_{10}]$ indexes to a tetragonal unit cell with $a = 3.8872(2)$ Å and $c = 29.263(2)$ Å.

(99) $Na_2[Sr_2Nb_2MnO_{10}]$ indexes to a tetragonal unit cell with $a = 3.9061(2)$ Å and $c = 28.891(1)$ Å.

(100) $H_2[Sr_2Nb_2MnO_{10}]$ was formed by stirring 1 g of $Bi_2O_2[Sr_2Nb_2MnO_{10}]$ in 6 M HCl for 3 days. $Na_2[Sr_2Nb_2MnO_{10}]$ was synthesized by reacting 0.5 g of $H_2[Sr_2Nb_2MnO_{10}]$ with 100 mL of 1 M NaOH at 60 °C for 3 days.

(101) $Na_2Eu_{1.33}La_{0.67}Ti_3O_{10}$, synthesized by traditional solid-state reaction of the constituent oxides and carbonates at 1100 °C, was reacted with 0.67 equiv of $Ca(NO_3)_2·4H_2O$ at 350 °C for 3 days to form $Ca_{0.67}Na_{0.67}Eu_{1.33}La_{0.67}Ti_3O_{10}$, which was subsequently reacted with 0.1 M HNO_3 at 45 °C for 2 days to form $Ca_{0.67}H_{0.67}Eu_{1.33}La_{0.67}Ti_3O_{10}$.

(102) JCPDF File No. 09-0127.

(103) (a) Iler, R. K. *J. Colloid Interface Sci.* **1966**, *21*, 569. (b) Kleinfeld, E. R.; Ferguson, G. S. *Science* **1994**, *265*, 370, (c) Fendler, J. H.; Meldrum, F. *Adv. Mater.* **1995**, *7*, 607. (d) Mallouk, T. E.; Kim, H.-N.; Ollivier, P. J.; Keller, S. W. In *Comprehensive Supramolecular Chemistry*; Alberti, G., Bein, T., Eds.; Elsevier Science: Oxford, UK, 1996; Vol. 7, pp 189−218. (e) Decher, G. *Science* **1997**, *277*, 1232.

(104) Schaak, R. E.; Mallouk, T. E., unpublished results.

(105) Uma, S.; Gopalakrishnan, J. *J. Solid State Chem.* **1993**, *102*, 332.

(106) Choy, J.-H.; Kim, J.-Y.; Kim, S.-J.; Sohn, J.-S.; Han, O. H. *Chem. Mater.* **2001**, *13*, 906.

(107) Goga, M.; Seshadri, R.; Ksenofontov, V.; Gutlich, P.; Tremel, W. *J. Chem. Soc., Chem. Commun.* **1999**, 979.

(108) For example, see (a) Adam, A.; Schuster, H.-U. *Z. Anorg. Allg. Chem.* **1990**, *584*, 150. (b) Ozawa, T. C.; Kauzlarich, S. M.; Bieringer, M.; Greedan, J. E. *Chem. Mater.* **2001**, *13*, 1804.

CM010689M